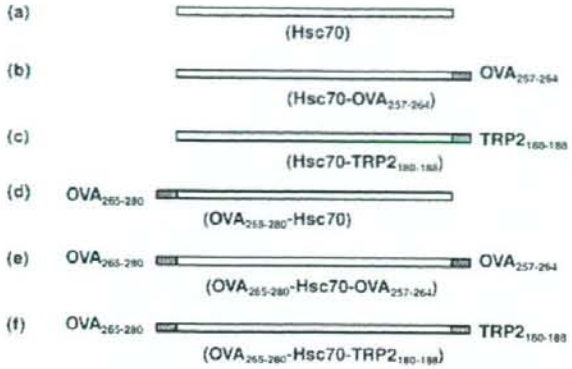

Fig. 1. Recombinant hsc70 and fusion proteins used in this study. Cytotoxic T lymphocyte epitopes $OVA_{257-264}$ and $TRP2_{180-188}$ were fused to the C-terminus of hsc70. (d–f) In some constructs, the helper T cell epitope $OVA_{265-280}$ was fused to the N-terminus of hsc70. Recombinant proteins also contained an N-terminal 6 × His-tag. They were expressed in *E. coli*, M15, and purified with Ni-NTA columns.

Reagents. Synthetic peptides $OVA_{265-280}$ (TEWTSSNVMEERKIKV), $OVA_{257-264}$ (SIINFEKL), and $TRP2_{180-188}$ (SVYDFFVWL) were purchased from Sawady (Tokyo, Japan). Their sequences were confirmed by a 490 Procise protein sequencer (Perkin-Elmer, Tokyo, Japan). Expression and purification of synthetic peptides fused with hsc70 were done as described previously.[11–14] Tetramer consisting of H-$2K^b$ plus SIINFEKL ($OVA_{257-264}$) labeled with phycoerythrin (PE) was purchased from MBL (Nagoya, Japan).

Preparation of recombinant fusion proteins. The recombinant hsc70 and fusion proteins described in Figure 1 were produced as previously described.[14] For the hsc70-$OVA_{257-264}$, hsc70-$TRP2_{180-188}$, $OVA_{265-280}$-hsc70, $OVA_{265-280}$-hsc70-$OVA_{257-264}$, and $OVA_{265-280}$-hsc70-$TRP2_{180-188}$, mini-genes encoding $OVA_{257-264}$, $TRP2_{180-188}$, and $OVA_{265-280}$ were amplified by polymerase chain reaction using forward or reverse primers containing 5′ *Bam*HI and 3′ *Kpn*I restriction sites and subcloned into the pQE31 vector (Qiagen, Germantown, MD, US). *Escherichia coli* (*E. coli*) strain M15 was transformed by the constructed plasmids and grown in Lysogeny broth (LB) medium containing ampicillin (50 μg/mL) and kanamycin (20 μg/mL). Protein expression was induced by 0.1 M isopropyl-β-D-thiogalactoside. The protein was solubilized in buffer B (8 M urea, 0.1 M sodium phosphate, 0.01 M Tris/HCl, pH 8.0) and, after centrifugation of the lysate at 10 000 *g*, the supernatant was applied to an $Ni^2 \pm$ NTA (nitrilotriacetic acid) agarose column and extensively washed with buffer C (8 M urea, 0.1 M sodium phosphate, 0.01 M Tris/HCl, pH 6.3). The $Ni^2 \pm$ NTA resin-bound 6× His-tagged protein was refolded rapidly by washing with 35 column volumes of urea-free Tris buffer (pH 7.5) and eluted with Tris buffer containing 200 mM imidazole. The eluate was extensively dialyzed against phosphate-buffered saline (PBS) (pH 7.4) to remove imidazole, and then it was concentrated using an Amicon Ultra-15 centrifugal filter device (Millipore, Bedford, MA, USA). The recovered proteins were subjected to Detoxi-gel Endotoxin Removing Columns (Pierce, Rockford, IL, USA) to get rid of contaminated endotoxin.

Vaccination and induction of CTL. C57BL/6 mice were vaccinated intraperitoneally twice in a 1-week interval with the indicated amount of synthetic peptides plus incomplete Freund's adjuvant (IFA) or with 10 μg (or the indicated dose) of hsc70 fusion protein. Two weeks after the second immunization, the mice were sacrificed and spleen cells were stimulated *in vitro* with each peptide at 10^{-6} M final concentration for 5 days.

^{51}Cr-release assay. The cytolytic activity of the induced CTL was determined by a standard ^{51}Cr-release assay. Target cells were labeled with 50 μCi ^{51}Cr-labeled sodium chromate in RPMI with 10% fetal calf serum for 1 h at 37°C and then washed twice with unsupplemented RPMI. Target cells (5×10^3) were added to titrated CTL effectors in 96-well round-bottom plates. Plates with final volume of 200 μL/well were centrifuged to promote cell contact and incubated at 37°C for 4 h. Then 100 μL of supernatant from each well was harvested manually and the radioactivity released into the supernatant was measured in a γ-counter. The percent specific release was calculated from the mean of duplicate cultures according to the following formula: percent specific ^{51}Cr release = (experimental release – spontaneous release) × 100/[maximal release (2% Triton X) – spontaneous release].

Enzyme-linked immunospot (ELISPOT) assay. For the ELISPOT assay, HA-Multiscreen plates (Millipore, Burlington, MA, USA) were coated with 50 μL of an antimouse γ-interferon (IFN-γ) antibody (10 μg/mL; RMMG1) in PBS, incubated overnight at 4°C, washed with PBS/0.25% Tween20 to remove unbound antibody and blocked with 100 μL/well PBS containing 5% bovine serum albumin for 1 h at 37°C. Immunized spleen cells were stimulated with 10^{-6} M peptide for 5 dyas and effector cells were obtained. The resulting cells (1×10^4 or 2×10^3 cells/well, 96-well plate) were incubated with mitomycin C (50 μg/mL for 45 min) treated, 5×10^5 naïve spleen cells/well pulsed with or without 1 μg/mL peptides in triplicate form. After incubation for 19 h at 37°C with 5% CO_2, the plates were extensively washed with PBS/0.25% Tween 20, and 100 μL/well biotinylated detecting antibody against mouse IFN-γ (1 μg/mL; R46A2) was added. After 2 h incubation at room temperature, the plates were washed with PBS/0.25% Tween 20, and 50 μL/well avidin solution (alkaline phosphatase conjugated) was added and incubated for 2 h. Spots were developed using nitro blue tetrazolium chloride/5-bromo-4-chloro-3-indolyl phosphate (NBT/BCIP) and counted using a zoom stereo microscope at ×40 magnification.

Depletion of CD8$^+$ cells by fluorescence-activated cell sorting (FACS). *In vitro* stimulated spleen cells with peptides were stained with fluorescein-isothiocyanate conjugated antimouse CD8α (53–6.7; eBioscience, San Diego, CA, USA). By using FACS Vantage, we sorted those stained cells into CD8$^-$ and CD8$^+$ cells. As a control, stimulated spleen cells were mock sorted and non-depleted effector cells were obtained. Those CD8$^+$ depleted and non-depleted cells were used for CTL assay and ELISPOT assay.

Immunotherapy of solid tumors. On day 0, mice were inoculated intradermally with 1×10^6 E.G7 cells on the right side of the back. On days –14 and –7, days 0 and 7, or days 2 and 9, mice were vaccinated with 10 μg hsc70 fusion proteins. Mice challenged with 2×10^5 MO5 cells were vaccinated with 10 μg hsc70 fusion proteins on days 0 and 7. Tumor size was measured every 2–3 days, and the average tumor diameter was determined. Average tumor diameter = [longest tumor diameter + shortest tumor diameter]/2.

Immunotherapy of lung metastases. On day 0, mice were inoculated with 5×10^5 MO5 cells via the tail vein. On days 0 and 2, or on days 2 and 9, those mice were vaccinated with 10 μg hsc70-$OVA_{257-264}$. On day 15, the mice were sacrificed and the metastatic spots on the lung surface were counted using a zoom stereo microscope (DSZT-44IF; Carton, Tokyo, Japan). In another experiment, MO5 inoculated mice were vaccinated with 10 μg hsc70 or hsc70-$OVA_{257-264}$ or $OVA_{265-280}$-hsc70-$OVA_{257-264}$ on days 0, 2, 5, and 7. On day 21, the mice were sacrificed, and the spots were counted. For CD4$^+$ cell depletion, on days –2, 0, 2, and 5, 100 μL GK1.5 (ascites, containing approximately 100 μg of antibody) was injected. Control mice were injected an equal volume of normal mouse ascites.

Immunotherapy of established tumor. On day 0, mice were inoculated intradermally with 1×10^6 E.G7 cells on the right

side of the back. On day 6, 2×10^6 OTI CD8$^+$ T cells were injected via tail vein, and simultaneously, 10 μg hsc70-$OVA_{257\text{-}264}$ or equal molar PA28α-$OVA_{257\text{-}264}$ was once peritoneally injected. For purification of OTI CD8$^+$ T cells, OTI splenocytes were at first depleted of CD11b cells with BD IMag antimouse CD11b Magnetic Particles-DM (negative selection) (BD Biosciences, San Jose, CA, USA) to remove splenic DC, and then, CD8$^+$ T cells were positively purified with BD IMag antimouse CD8 Magnetic Particles-DM (positive selection). Tumor diameter was monitored every 2–3 days. The average tumor diameter was determined. Average tumor diameter = [longest tumor diameter + shortest tumor diameter]/2.

Proliferation of transferred T cells. Purified OTI CD8$^+$ T cells were stained with 5 μM carboxyfluorescein succinimidyl ester (CFSE) (Dojindo, Kumamoto, Japan). CFSE-labeled 2×10^6 OTI CD8$^+$ T cells were adoptively transferred into C57BL/6 mice via tail vein, and simultaneously vaccinated with 10 μg hsc70-$OVA_{257\text{-}264}$ or equal molar PA28α-$OVA_{257\text{-}264}$ via the peritoneal cavity. Control mice were not injected with any proteins. Three days later, splenocytes of those recipients were stained with PE-conjugated antimouse CD44 (IM7; eBioscience) as a T-cell activated marker, and then division of OTI CD8$^+$ T cells was determined by CFSE dilution.

Results

Generation of CTL by hsc70 fusion proteins. Diagrams of the fusion proteins used in this study are shown in Figure 1. The H-2K^b epitopes $OVA_{257\text{-}264}$ and $TRP2_{180\text{-}188}$ were genetically fused to the carboxyl terminus of hsc70 (Fig. 1). In addition, a presumed helper epitope $OVA_{265\text{-}280}$ that was previously suggested to augment $OVA_{257\text{-}264}$ specific CD8$^+$ T cell by DNA vaccination[15] was fused to the amino terminus of hsc70 alone or hsc70 containing C-terminal epitopes (Fig 1e,f). Fusion proteins were expressed in *E. coli* and recombinant proteins were purified as described previously.[14] The endotoxin level in these proteins was less than 0.5 EU/mg as determined by the Limulus ES test (Mitsubishi Chemical Medicine Corporation, Tokyo, Japan).

We first investigated whether CD8$^+$ cytotoxic T lymphocytes were generated by vaccination with hsc70 fused with both $OVA_{257\text{-}264}$ and $OVA_{265\text{-}280}$. Mice were vaccinated twice in a 1-week interval with 10 μg hsc70 fusion protein, and 2 weeks later after the final imminization, spleen cells were stimulated with 10^{-6} M $OVA_{257\text{-}264}$ peptide for 5 days, and the resulting $OVA_{257\text{-}264}$-specific CTL were confirmed by staining with tetramer comprising H-2K^b + SIINFEKL ($OVA_{257\text{-}264}$) peptide, standard ^{51}Cr-release assay, and cytokine ELISPOT assay. We identified CD8$^+$, tetramer positive cells by FACS analysis (Fig. 2a, upper panel). The CD8$^+$ T cells killed EL-4 cells pulsed with $OVA_{257\text{-}264}$ peptide, as well as E.G7 cells that express full length OVA, but not EL4 cells (Fig. 2b) and showed IFN-γ production as determined by ELISPOT assay (Fig. 2b). The cytotoxicity and IFN-γ-producing activities were abrogated (Fig. 2a,b) by the depletion of CD8$^+$ T cells by FACS (Fig. 2a, lower panel). *In vivo* cross-priming ability was caused by fusion of hsc70 but not by other self proteins, because a proteasome activator, PA28α fused with $OVA_{257\text{-}264}$ showed only marginal CTL generation as we previously demonstrated,[14] and induced only partial proliferation of CFSE-labeled CD8$^+$ T cells purified from OTI TCR transgenic mice (Fig. 10b-3).

Next, we investigated CTL generation by immunization with hsc70 fusion proteins and synthetic peptides, $OVA_{257\text{-}264}$ and $OVA_{265\text{-}280}$, in an emulsion of IFA as described in Figure 2. Mice were immunized twice in a 1-week interval with 1 μg of synthetic $OVA_{257\text{-}264}$ peptide plus IFA, or with 10 μg of the fusion proteins. Two weeks after the second immunization, spleen cells

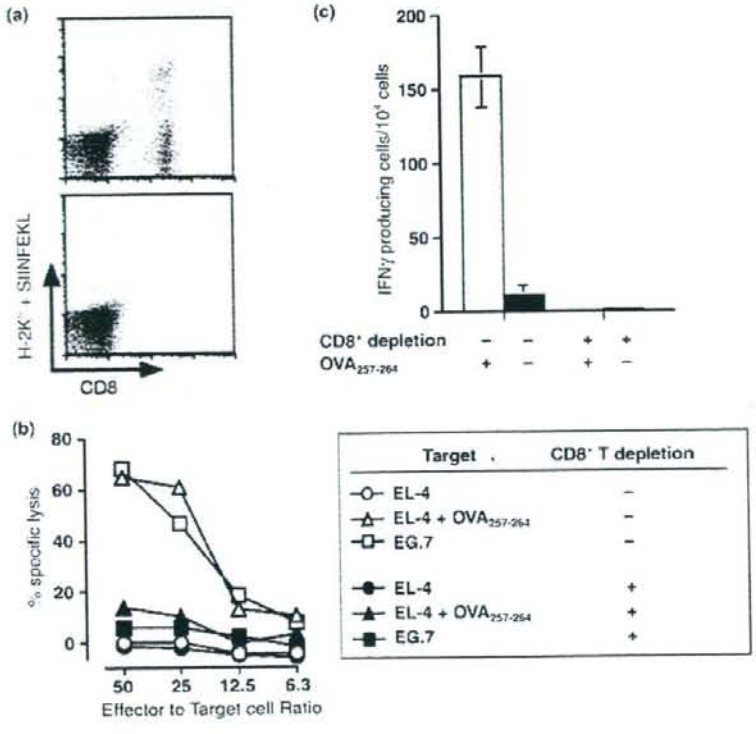

Fig. 2. Generation of CD8$^+$ CTL specific to $OVA_{257\text{-}264}$ by vaccination with hsc70 fusion protein. C57BL/6 mice were immunized intraperitoneally with 10 μg $OVA_{265\text{-}280}$-hsc70-$OVA_{257\text{-}264}$ twice in a 1-week interval. Two weeks after the second immunization, the spleen cells were stimulated *in vitro* with 10^{-6} M $OVA_{257\text{-}264}$ for 5 days. (a, upper panel) The resulting cells were stained with tetramer consisting of H-2K^b and $OVA_{257\text{-}264}$ (MBL, Nagoya, Japan). (a, lower panel) CD8$^+$ cells were sorted out by fluorescence-activated cell sorting (FACS) Vantage. Cells in (a) were used for ^{51}Cr-release assay (b) and cytokine ELISPOT assay (c), as indicated.

doi: 10.1111/j.1349-7006.2008.00788.x

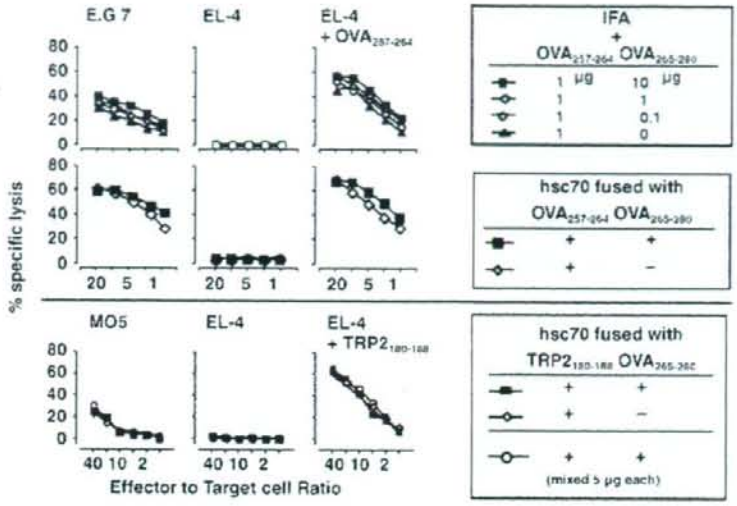

Fig. 3. Comparison of the efficiency of cytotoxic T lymphocyte (CTL) generation by vaccination with hsc70 fusion proteins or synthetic peptides. C57BL/6 mice were immunized intraperitoneally with the indicated doses of synthetic peptides plus incomplete Freund's adjuvant (IFA) or with 10 μg (or the indicated volume) hsc70 fusion proteins, twice in a 1-week interval. Two weeks after the second immunization, the spleen cells were stimulated *in vitro* with 10^{-6} M $OVA_{257-264}$ or $TRP2_{180-188}$ for 5 days. CTL activity against E.G7, EL4, and EL4 pulsed with $OVA_{257-264}$ was examined using a standard ^{51}Cr-release assay.

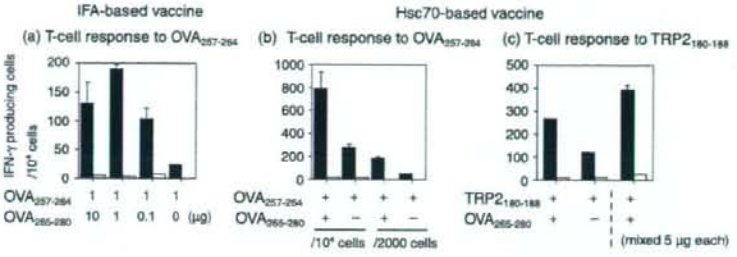

Fig. 4. Enzyme-linked immunospot assay for cytotoxic T lymphocyte (CTL) generated by immunization with peptides or hsc70 fusion proteins. The number of γ-interferon (IFN-γ)–producing cells in spleens of mice immunized with peptides or fusion proteins was determined. The same protocol for *in vivo* immunization and *in vitro* peptide stimulation was used as for Figure 2. Stimulated spleen cells (1×10^4 or 2×10^3 cells/well, 96-well plate) were incubated with 5×10^5 naïve spleen cells/well pulsed with (black bar) or without (white bar) 1 μg/mL $OVA_{257-264}$ or TRP2 $_{180-188}$ in triplicate form for 19 h. IFA, incomplete Freund's adjuvant.

were stimulated with 10^{-6} M $OVA_{257-264}$ peptide for 5 days, and the resulting CTL activity was examined with a standard ^{51}Cr-release assay. Peptide immunization generated CTL that killed E.G7 and EL4 pulsed with $OVA_{257-264}$ but not EL4. Simultaneous immunization with graded doses of $OVA_{265-280}$ slightly enhanced the CTL activity in a dose-dependent manner (Fig. 3, top row). Immunization with 10 μg hsc70 fusion proteins, corresponding to only one-tenth the molar ratio used for peptide vaccination, generated even higher cytolytic activity toward E.G7 and EL4 pulsed with $OVA_{257-264}$ and marginal enhancement was observed with $OVA_{265-280}$-hsc70-$OVA_{257-264}$ compared to hsc70-$OVA_{257-264}$ (Fig. 3, middle row). These results indicate that hsc70, although a ubiquitously expressed self-antigen in the host, has a powerful adjuvant effect over that of IFA. Not only hsc70-$OVA_{257-264}$ but also hsc70-$TRP2_{180-188}$ induced peptide-specific CTL. It was noted that hsc70-$TRP2_{180-188}$-induced CTL could kill MO5 melanoma cells spontaneously expressing TRP2 at the higher E/T ratio. But we observed no enhancement of cytolysis to $TRP2_{180-188}$ by immunization with $OVA_{265-280}$-hsc70-$TRP2_{180-188}$, compared to hsc70-$TRP2_{180-188}$ (Fig. 3, bottom row).

ELISPOT assay for CTL generated by hsc70 fusion proteins. The effect of a helper epitope, $OVA_{265-280}$ in stimulating the generation of peptide specific CTL was difficult to evaluate using a standard ^{51}Cr-release assay. For this reason, we next carried cytokine ELISPOT assays to examine whether a more sensitive technique would reveal differences in the immunization strategies. The same protocol for *in vivo* immunization and *in vitro* peptide stimulation was used as in Figure 3. ELISPOT assays showed a clear effect of the $OVA_{265-280}$ helper epitope in a dose-dependent manner with both IFA-peptide and hsc70 fusion protein immunization (Fig. 4b,c). The number of IFN-γ producing cells was much higher in hsc70 fusion proteins, which was consistent with the results obtained in the ^{51}Cr-release assay. We could still observe the enhanced helper-effect of $OVA_{265-280}$ by immunization with the heterologous combination of $OVA_{265-280}$-hsc70-$TRP2_{180-188}$ (Fig. 4c). Intriguingly, administration of a mixture of hsc70-$TRP2_{180-188}$ and $OVA_{265-280}$-hsc70 gave rise to a higher number of spots than hsc70-$TRP2_{180-188}$ alone (Fig. 4c), suggesting that these hsc70 fusion proteins were targeted to the same specialized antigen presenting cells *in vivo* through putative cell surface receptors like CD91 or LOX-1.[7,8] Taken together, these data suggest that addition of a helper epitope to the hsc70-CTL epitope complex increased the population of peptide-specific CTL.

***In vivo* protection effect of hsc70 fusion proteins against intradermal tumor growth.** To gain insight into *in vivo* protection effect of the hsc70 fusion proteins, we vaccinated syngeneic mice at days –14 and –7, days 0 and 7, or days 2 and 9 and monitored the growth of E.G7 inoculated intradermally on day 0. On vaccination at days –14 and –7 or days 0 and 7, hsc70-$OVA_{257-264}$ showed apparent protection, regardless of the presence of the helper epitope (Fig. 5a,b). However, the days 2 and 9 vaccination regimine did not show any protective effect (Fig. 5c), indicating that the vaccine is not strong enough to cure tumors once they have been established in the hosts.

Next, we inoculated the OVA expressing B16 melanoma MO5 to examine the effect of hsc70 fusion proteins in another tumor model. Although K^b expression is difficult to detect by FACS analysis (data not shown), vaccination with

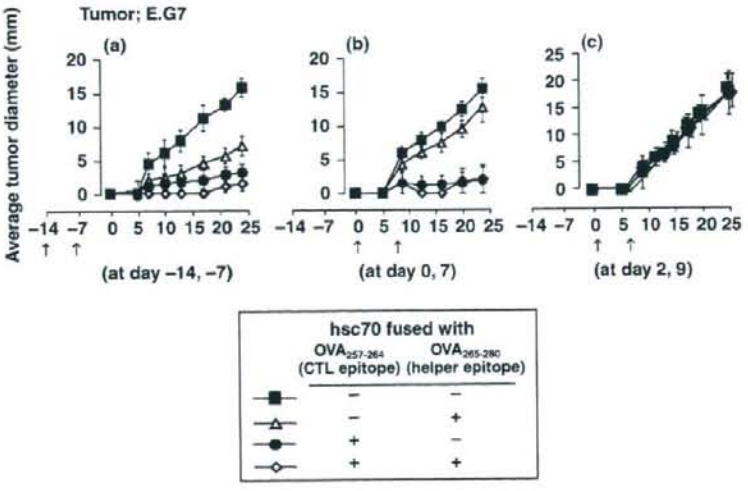

Fig. 5. *In vivo* antitumor effect of hsc70 fusion proteins against E.G7. C57BL/6 mice were vaccinated intraperitoneally with 10 μg of each hsc70 fusion protein as indicated on (a) days −14 and −7, (b) days 0 and 7, or (c) days 2 and 9. The mice were challenged with E.G7 at day 0 and then tumor growth was monitored. (n = 5). CTL, cytotoxic T lymphocyte.

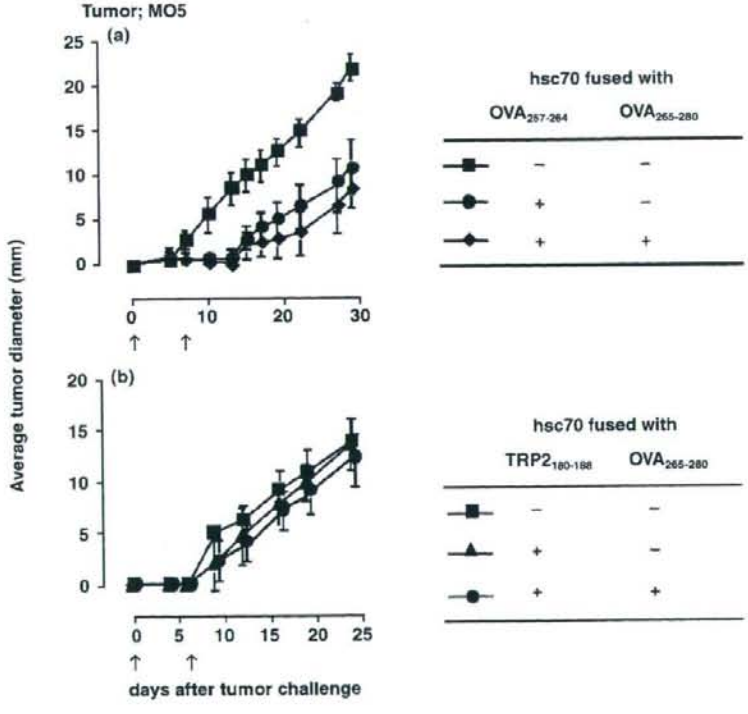

Fig. 6. *In vivo* antitumor effect of hsc70 fusion proteins against MO5. C57BL/6 mice were vaccinated intraperitoneally with 10 μg of each hsc70 fusion protein as indicated on days 0 and 7. Mice were challenged with MO5 at day 0 and tumor growth was monitored (n = 5).

hsc70-$OVA_{257\text{-}264}$ on days 0 and 7 significantly delayed the appearance of the tumor, and inclusion of the $OVA_{265\text{-}280}$ helper epitope had a marginally additive effect (Fig. 6a). By contrast, hsc70-$TRP2_{180\text{-}188}$ did not show significant protection, demonstrating that the vaccine effect of hsc70 depends on the antigenic peptides used in the fusion protein.

***In vivo* protection effect of hsc70 fusion proteins against melanoma metastasis.** The induction of tumor immunity by any vaccination strategy has two aspects, (i) the remission of the original tumor mass; and (ii) the prevention/elimination of metastatic lesions. To examine the effect of hsc70 fusion proteins on the later, we injected MO5 melanoma cells intravenously in a standard metastasis model and vaccinated with hsc70-$OVA_{257\text{-}264}$ at days 0 and 7 or at days 2 and 9. The numbers of pigmented metastatic spots on the lung surface were counted on day 15 after sacrificing the mice. The average spot number without vaccination was 70.6. In contrast, vaccination at days 0 and 7 and days 2 and 9 resulted in 17 and 61.2 spots, respectively (Fig. 7a), indicating that hsc70-$OVA_{257\text{-}264}$ suppressed the MO5 metastasis. Next, we immunized mice with hsc70-$OVA_{257\text{-}264}$

doi: 10.1111/j.1349-7006.2008.00788.x

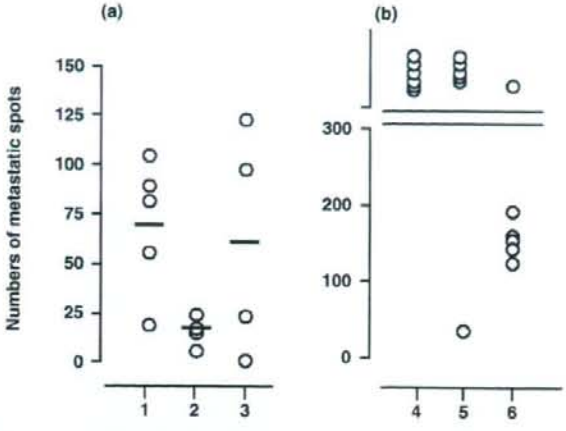

Fig. 7. *In vivo* antitumor effect of hsc70 fusion proteins against MO5 lung metastasis. (a) On day 0, mice were challenged with MO5 via the tail vein, and vaccinated with hsc70-$OVA_{257-264}$ at days 0 and 7 (column 2) or at days 2 and 9 (column 3). The numbers of metastatic spots of the lung surface were counted on day 15 after sacrificing the mice. Control mice were not vaccinated (column 1) (n = 4 or 5). (b) Mice were immunized with hsc70-$OVA_{257-264}$ (column 5) and $OVA_{265-280}$-hsc70-$OVA_{257-264}$ (column 6) at days 0, 2, 5, and 7, and the spot numbers of lungs, were counted at day 21. Control mice were not vaccinated (column 4) (n = 6).

and $OVA_{265-280}$-hsc70-$OVA_{257-264}$ on days 0, 2, 5, and 7, and the number of lung spots were counted at day 21. $OVA_{265-280}$-hsc70-$OVA_{257-264}$ significantly suppressed metastasis, while on the other hand, hsc70-$OVA_{257-264}$ showed no protection (Fig. 7b), indicating that addition of the $OVA_{265-280}$-helper epitope to hsc70-$OVA_{257-264}$ significantly enhanced the protection against MO5 lung metastasis. Representative pictures of the lung metastasis are shown in Figure 8a,b, in which the figure designations correspond to those of Figure 7. We confirmed that hsc70 alone gave no protection against MO5 metastasis, whereas $OVA_{265-280}$-hsc70-$OVA_{257-264}$ reproducibly suppressed the metastasis as shown in Figure 8c.

In order to analyze effect of $CD4^+$ T cells, we injected anti-CD4 mAb to eliminate *in vivo* before vaccination with $OVA_{265-280}$-hsc70-$OVA_{257-264}$, and monitored metastatic spots. $CD4^+$ T cell depletion slightly reduced the vaccination effect of $OVA_{265-280}$-hsc70-$OVA_{257-264}$ (Fig. $9a_{2,3}$,$b_{2,3}$) and the effect was nearly comparable for that of hsc70-$OVA_{257-264}$ (Fig. $9a_{3,4}$,$b_{3,4}$).

An immune therapy for established tumors by hsc70 fusion protein. One of the goals of hsc70 fusion proteins is an immune therapy for established tumors *in vivo*. Since vaccination at day 6 after E.G7 inoculation did not show eradication of the tumor (data not shown), we simultaneously injected 2×10^6 OTI-derived, purified $CD8^+$ T cells, in addition to hsc70-$OVA_{257-264}$, to tumor-bearing mice. As a control, PA28α-$OVA_{257-264}$ was injected. Adoptively transferred OTI $CD8^+$ T cells alone or with an injection of PA28α-$OVA_{257-264}$ did not confer tumor regression; however, OTI $CD8^+$ T cells plus hsc70-$OVA_{257-264}$ completely rejected once-established tumor masses (Fig. 10a). We observed vigorous proliferation of adoptively transferred CFSE-labeled OTI $CD8^+$ T cells in the spleen after vaccination with hsc70-$OVA_{257-264}$ but not by PA28α-$OVA_{257-264}$ (Fig. 10b). We also observed by FACS the proliferating CFSE-labeled OTI $CD8^+$ T cells in the regional lymph node and tumor tissues (data not shown), suggesting that infiltration of activated OTI $CD8^+$ T cells into the tumor mass is important for tumor rejection.

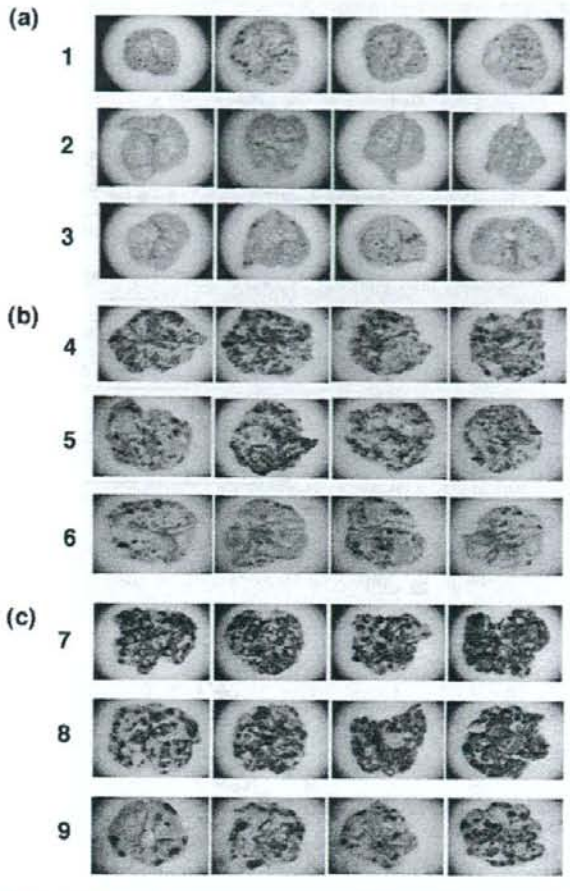

Fig. 8. Macroscopic visualization of lung metastases. Metastatic spots on lung surfaces were observed with zoom stereo microscope at ×10 magnification. (a,b) The designations correspond to those in Figure 7. (c) On day 0, mice were challenged with MO5 via the tail vein, and vaccinated with hsc70 (column 8) or $OVA_{265-280}$-hsc70-$OVA_{257-264}$ (column 9) at days 0, 2, 5, and 7. At day 21, mice were sacrificed, and the spots were quantified. Control mice were not vaccinated (column 7).

Discussion

HSP are evolutionally conserved across species and are constitutively expressed in all cells. Their expression level is dramatically increased by heat shock, a phenomenon termed the heat shock response. Heat shock response is caused not only by heat but also by other stresses such as heavy metals, hypoxia, alcohol intoxication, glucose starvation, and even cytokine stimulation.[16] HSP stimulate proper folding of proteins damaged by these stressors and thus constitute a protein salvage system. On the other hand, it was recently suggested that HSP are also linked to the ubiquitin-proteasome pathway to degrade proteins.

Hsp90 and hsc70 recognize unfolded proteins and peptides in the cytosol, where they recruit the E3 ubiquitin ligase CHIP (carboxyl terminus of hsc70 interacting protein) to polyubiquitinylate these substrates.[17,18] The polyubiquitinylated proteins are degraded by the 26S proteasome, and some of the degradation products can potentially serve as peptide ligands for MHC class I molecules.

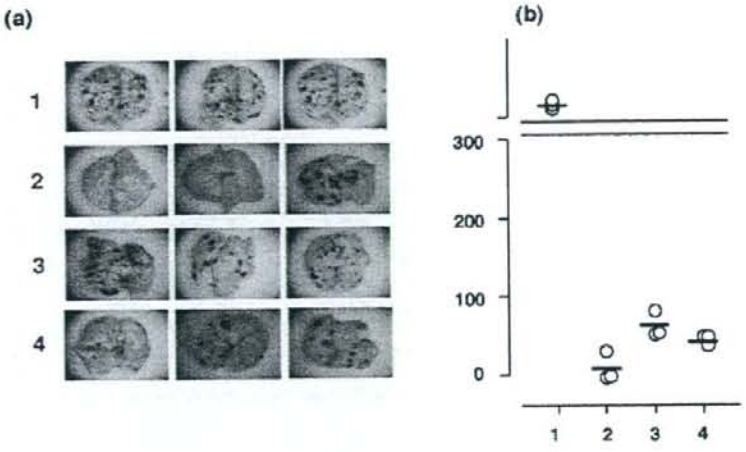

Fig. 9. Effect of CD4+ cell depletion on vaccination against MO5 lung metastasis. On day −2, 0, 2, and 5, mice were injected with control mouse ascites (column 1, 2, and 4) or GK1.5 (anti-CD4) ascites (column 3). On day 0, mice were challenged with MO5 via the tail vein, and vaccinated with $OVA_{265-280}$-hsc70-$OVA_{257-264}$ (column 2,3) and hsc70-$OVA_{257-264}$ (column 4) at days 0, 2, 5, and 7. Control mice were not vaccinated (column 1). (a) Metastatic spots on lung surfaces were observed as in Figure 8. (b) The numbers of metastatic spots were counted on day 21 after sacrificing the mice. (n = 3).

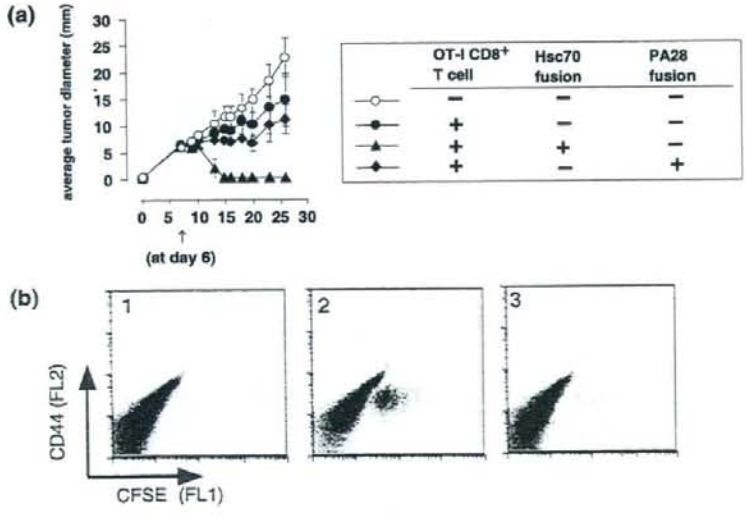

Fig. 10. An immune therapy by hsc70 fusion protein for established tumor. (a) On day 0, mice were challenged with a 1×10^6 E.G7 tumor. At day 6, 2×10^6 OTI CD8+T cells were injected via tail vein, and simultaneously, 10 μg hsc70-$OVA_{257-264}$ or equal molar PA28α-$OVA_{257-264}$ was once peritoneally injected. Tumor diameter was monitored every 2–3 days. (n = 4). (b) Carboxyfluorescein succinimidyl ester (CFSE)–labeled 2×10^6 OTI CD8+T cells were adoptively transferred into C57BL/6 mice and simultaneously vaccinated with 10 μg hsc70-$OVA_{257-264}$ (panel 2) or equal molar PA28α-$OVA_{257-264}$ (panel 3). Control mice were not injected with any proteins (column 1). Three days later, proliferating OTI CD8+ T cells in the spleen were investigated by carboxyfluorescein succinimidyl ester dilution (CFSE) and CD44.

The proteins and peptides bound to HSP, once released outside cells, are efficiently trapped by antigen-presenting cells via a number of HSP receptors and can then be cross presented to CD8+ T cells in the context of MHC class I molecules.[19] In this context, mild biochemical procedures for the purification of HSP from tumor cells allow the copurification of unknown tumor antigens bound to HSP, which is the rationale behind the use of antigen-HSP complexes for cancer vaccine therapy without knowing the identity of the tumor antigens recognized by T cells. One disadvantage of this vaccine approach may be the quantity of tumor antigens bound to HSP. Thus, many HSP isolated from tumor cells seem to lack associated tumor antigens.[4] Fusion of mini genes encoding T cell epitopes to HSP cDNAs to construct a fusion protein may be a solution to this problem. Indeed, we previously found efficient generation of CTL by vaccination with several epitopes fused to hsc70.[11] A question that remained to be addressed was whether this type of vaccine could eradicate tumors *in vivo*. In the present study, we have demonstrated that vaccination with a CD8+ T cell epitope fused to hsc70 resulted in a significant protective effect against *in vivo* tumor growth, and that simultaneous fusion of an epitope recognized by CD4+ T cells to HSP increased the population of primed CD8+ T cells, resulting in enhanced eradication of tumors.

Although antigens are readily cross-presented to CTL *in vitro* by DC or other antigen presenting cells pulsed with HSP-epitope complexes, these results do not necessarily imply that administration of these HSP-epitope complexes *in vivo* will generate CTL efficiently enough to eradicate tumors. In order to obtain *in vivo* protection, T cells need to be fully activated, which can be accomplished by suitable activation of DC with HSP. Hsp70 and Gp96 have been shown to interact with toll-like receptors 4 and 2 (TLR4 and 2),[5,20] an encounter that activates DC to fully prime T cells. However, the idea that DC can be activated with HSP is still controversial.[21] Endotoxin contaminating of the recombinant proteins, even though rigorously removed, might, at least in part, participate in activation of DC.[22,23] On the other hand, Datta *et al.* showed that among agonists for various TLR, only those for TLR3,7 and 9 but not for TLR2 and 4, enabled DC to cross-prime CD8+ T cells.[24] We also observed that cross-priming by hsp70 fusion proteins

doi: 10.1111/j.1349-7006.2008.00788.x

occurs equally well *in vivo*, even in TLR2 and 4 double KO mice (data not shown). These results suggest that the effect of endotoxin contamination is minimum or negligible in cross-priming. It is possible that interaction between CD40 and hsp70 activates DC, as previously demonstrated.[25]

Addition of a $CD4^+$ T cell epitope to the hsc70-CTL epitope augmented the vaccination effect, especially in the MO5 lung metastasis model (Figs 7–9). This effect apparently resulted from an increased population of IFN-γ-producing $CD8^+$ T cells as determined by ELISPOT assay (Fig. 4). Both helper and CTL epitopes should be expressed on the same DC because the two epitopes are within a single hsc70 molecule. Therefore, there may be simultaneous activation of both $CD4^+$ and $CD8^+$ T cells on the surface of a single DC. Activated $CD4^+$ T cells express CD40L, which can interact with CD40 on DC. Thus, conditioning of DCs by $CD4^+$ T cells is a likely possibility, and this might provoke much more efficient activation of $CD8^+$ T cells *in vivo*.[26,27] Along this line, we attempted to generate $OVA_{265-280}$ specific $CD4^+$ T cells *in vitro* by peptide stimulation but were unsuccessful.

From a clinical viewpoint, it is important to successfully produce a fusion protein containing hsc70 together with an epitope from a human cancer antigen. In this context, we recently demonstrated that ESO p157–165 of NY-ESO-1, a cancer/testis antigen, fused to human hsc70, was cross-presented by DC to specific CTL clone, although the hsc70 preparation did not induce maturation of DC.[28] Moreover, repetitive stimulation of $CD8^+$ T cells with human DC pulsed with the fusion protein generated CTL against ESO p157–165. Taken together, the use of HSP-peptide complexes for cancer vaccination is a reasonable approach, not only from theoretical and practical perspectives.

Acknowledgments

The authors are grateful to Ms. Hiroiwa for recombinant protein preparations. This work was supported by grants-in-aid for Scientific Research on Priority Areas from the Ministry of Education, Culture, Sports, Science, and Technology of Japan.

References

1 Udono H, Srivastava PK. Heat shock protein 70-associated peptides elicit specific cancer immunity. *J Exp Med* 1993; **178**: 1391–6.
2 Udono H, Srivastava PK. Comparison of tumor-specific immunogenicities of stress-induced proteins gp96, hsp90, and hsp70. *J Immunol* 1994; **152**: 5398–403.
3 Tamura Y, Peng P, Liu K, Daou M, Srivastava PK. Immunotherapy of tumors with autologous tumor-derived heat shock protein preparation. *Science* 1997; **278**: 117–20.
4 Ishii T, Udono H, Yamano T *et al.* Isolation of MHC class I-restricted tumor antigen peptide and its precursors associated with heat shock proteins hsp70, hsp90, and gp96. *J Immunol* 1999; **162**: 1303–9.
5 Asea A, Kraeft SK, Kurt-Jones EA *et al.* HSP70 stimulates cytokine production through a CD14-dependant pathway, demonstrating its dual role as a chaperone and cytokine. *Nat Med* 2000; **6**: 435–42.
6 Asea A, Rehli M, Kabingu E *et al.* Novel signal transduction pathway utilized by extracellular HSP70: role of toll-like receptor (TLR) 2 and TLR4. *J Biol Chem* 2002; **277**: 15028–34.
7 Binder RJ, Han DK, Srivastava PK. CD91: a receptor for heat shock protein gp96. *Nat Immunol* 2000; **1**: 151–5.
8 Delneste Y, Magistrelli G, Gauchat J *et al.* Involvement of LOX-1 in dendritic cell-mediated antigen cross-presentation. *Immunity* 2002; **17**: 353–62.
9 Berwin B, Hart JP, Rice S *et al.* Scavenger receptor-A mediates gp96/GRP94 and calreticulin internalization by antigen-presenting cells. *Embo J* 2003; **22**: 6127–36.
10 Ackerman AL, Giodini A, Cresswell P. A role for the endoplasmic reticulum protein retrotranslocation machinery during crosspresentation by dendritic cells. *Immunity* 2006; **25**: 607–17.
11 Udono H, Yamano T, Kawabata Y, Ueda M, Yui K. Generation of cytotoxic T lymphocytes by MHC class I ligands fused to heat shock cognate protein 70. *Int Immunol* 2001; **13**: 1233–42.
12 Udono H, Levey DL, Srivastava PK. Cellular requirements for tumor-specific immunity elicited by heat shock proteins: tumor rejection antigen gp96 primes $CD8^+$ T cells in vivo. *Proc Natl Acad Sci USA* 1994; **91**: 3077–81.
13 Suzue K, Young RA. Adjuvant-free hsp70 fusion protein system elicits humoral and cellular immune responses to HIV-1 p24. *J Immunol* 1996; **156**: 873–9.
14 Udono H, Saito T, Ogawa M, Yui K. Hsp-antigen fusion and their use for immunization. *Methods* 2004; **32**: 21–4.
15 Maecker HT, Umetsu DT, DeKruyff RH, Levy S. Cytotoxic T cell responses to DNA vaccination: dependence on antigen presentation via class II MHC. *J Immunol* 1998; **161**: 6532–6.
16 Lindquist S. The heat-shock response. *Annu Rev Biochem* 1986; **55**: 1151–91.
17 Connell P, Ballinger CA, Jiang J *et al.* The co-chaperone CHIP regulates protein triage decisions mediated by heat-shock proteins. *Nat Cell Biol* 2001; **3**: 93–6.
18 Murata S, Minami Y, Minami M, Chiba T, Tanaka K. CHIP is a chaperone-dependent E3 ligase that ubiquitylates unfolded protein. *EMBO Rep* 2001; **2**: 1133–8.
19 Binder RJ, Srivastava PK. Peptides chaperoned by heat-shock proteins are a necessary and sufficient source of antigen in the cross-priming of $CD8^+$ T cells. *Nat Immunol* 2005; **6**: 593–9.
20 Vabulas R, Braedel S, Hilf N *et al.* The endoplasmic reticulum-resident heat shock protein Gp96 activates dendritic cells via the Toll-like receptor 2/4 pathway. *J Biol Chem* 2002; **277**: 20847–53.
21 Tsan MF, Gao B. Endogenous ligands of Toll-like receptors. *J Leukoc Biol* 2004; **76**: 514–9.
22 Bausinger H, Lipsker D, Ziylan U *et al.* Endotoxin-free heat-shock protein 70 fails to induce APC activation. *Eur J Immunol* 2002; **32**: 3708–13.
23 Warger T, Hilf N, Rechtsteiner G *et al.* Interaction of TLR2 and TLR4 ligands with the N-terminal domain of Gp96 amplifies innate and adaptive immune responses. *J Biol Chem* 2006; **281**: 22545–53.
24 Datta SK, Redecke V, Prilliman KR *et al.* A subset of Toll-like receptor ligands induces cross-presentation by bone marrow-derived dendritic cells. *J Immunol* 2003; **170**: 4102–10.
25 Wang Y, Kelly CG, Karttunen JT *et al.* CD40 is a cellular receptor mediating mycobacterial heat shock protein 70 stimulation of CC-chemokines. *Immunity* 2001; **15**: 971–83.
26 Schoenberger SP, Toes RE, van der Voort EI, Offringa R, Melief CJ. T-cell help for cytotoxic T lymphocytes is mediated by CD40–CD40L interactions. *Nature* 1998; **393**: 480–3.
27 Ridge JP, Di Rosa F, Matzinger P. A conditioned dendritic cell can be a temporal bridge between a $CD4^+$ T-helper and a T-killer cell. *Nature* 1998; **393**: 474–8.
28 Susumu S, Nagata Y, Ito S *et al.* Cross-presentation of NY-ESO-1 cytotoxic T lymphocyte epitope fused to human heat shock cognate protein 70 by dendritic cells. *Cancer Sci* 2008; **99**: 107–12.

PARINT-00617; No of Pages 7

Parasitology International xxx (2008) xxx–xxx

Contents lists available at ScienceDirect

Parasitology International

journal homepage: www.elsevier.com/locate/parint

Rhoptry neck protein RON2 forms a complex with microneme protein AMA1 in *Plasmodium falciparum* merozoites☆

Jun Cao [a,b], Osamu Kaneko [a,c,*], Amporn Thongkukiatkul [d], Mayumi Tachibana [a], Hitoshi Otsuki [a], Qi Gao [b], Takafumi Tsuboi [e,f], Motomi Torii [a]

[a] Department of Molecular Parasitology, Ehime University Graduate School of Medicine, Shitsukawa, Toon, Ehime 791-0295, Japan
[b] Malaria Department, Jiangsu Institute of Parasitic Diseases, Meiyuan, Wuxi, Jiangsu 214064, People's Republic of China
[c] Department of Protozoology, Institute of Tropical Medicine (NEKKEN), Nagasaki University, Sakamoto, Nagasaki 852-8523, Japan
[d] Department of Biology, Faculty of Science, Burapha University, Chonburi 20131, Thailand
[e] Cell-Free Science and Technology Research Center, Ehime University, Matsuyama, Ehime 790-8577, Japan
[f] Venture Business Laboratory, Ehime University, Matsuyama, Ehime 790-8577, Japan

ARTICLE INFO

Article history:
Received 12 August 2008
Received in revised form 15 September 2008
Accepted 18 September 2008
Available online xxxx

Keywords:
AMA1
Erythrocyte invasion
Merozoite
Plasmodium falciparum
Rhoptry

ABSTRACT

Erythrocyte invasion is an essential step in the establishment of host infection by malaria parasites, and is a major target of intervention strategies that attempt to control the disease. Recent proteome analysis of the closely-related apicomplexan parasite, *Toxoplasma gondii*, revealed a panel of novel proteins (RONs) located at the neck portion of the rhoptries. Three of these proteins, RON2, RON4, and RON5 have been shown to form a complex with the microneme protein Apical Membrane Protein 1 (AMA1). This complex, termed the Moving Junction complex, localizes at the interface of the parasite and the host cell during the invasion process. Here we characterized a RON2 ortholog in *Plasmodium falciparum*. *Pf*RON2 transcription peaked at the mature schizont stage and was expressed at the neck portion of the rhoptry in the merozoite. Co-immunoprecipitation of *Pf*RON2, *Pf*RON4 and *Pf*AMA1 indicated that the complex formation is conserved between *T. gondii* and *P. falciparum*, suggesting that co-operative function of the rhoptry and microneme proteins is a common mechanism in apicomplexan parasites during host cell invasion. *Pf*RON2 possesses a region displaying homology with the rhoptry body protein *Pf*RhopH1/Clag, a component of the RhopH complex. However, here we present co-immunoprecipitation studies which suggest that *Pf*RON2 is not a component of the RhopH complex and has an independent role. Nucleotide polymorphism analysis suggested that *Pf*RON2 was under diversifying selective pressure. This evidence suggests that RON2 appears to have a fundamental role in host cell invasion by apicomplexan parasites, and is a potential target for malaria intervention strategies.

1. Introduction

Malaria is one of the most prevalent and deadly global infectious diseases, more than half of the world's population is at the risk of infection, and over 300 million people develop clinical disease each year of which 2 million are fatal [1]. Clinical malaria results from the replication of protozoan parasites of the genus *Plasmodium* in the circulating erythrocytes of the host. During the time between release from a rupturing mature schizont-infected erythrocyte and invasion of new erythrocytes, merozoites are transiently exposed in the circulation, and are thus potentially vulnerable to attack by preventive measures based upon immunological or biochemical methods. To design such tools, it is important to understand the molecular composition of the merozoite and the structure-function makeup of the molecular interactions that occur as the merozoite recognizes and gains entry into a host cell.

Like most apicomplexan parasites, the malaria merozoite invades host cells via a multistep process initiated by reversible binding to the erythrocyte surface. Subsequently, a high affinity attachment occurs between the apical end of the merozoite and the host cell, followed by the movement of the junctional adhesion zone (moving junction) around the merozoite toward its posterior pole. Finally the merozoite invaginates into the erythrocyte by forming a nascent parasitophorous vacuole [2]. The moving junction is one of the most distinctive features of apicomplexan invasion and was first observed in

Abbreviations: aa, amino acid(s); Ab, antibody; AMA1, apical membrane antigen 1; GST, Glutathione S transferase; PBS, phosphate-buffered saline; PCR, polymerase chain reaction; RON, rhoptry neck protein.

☆ Sequence data from this article have been deposited with the GenBank™/EMBL/DDBJ databases under accession numbers AB444588–AB444592.

* Corresponding author. Department of Protozoology, Institute of Tropical Medicine (NEKKEN), Nagasaki University, Sakamoto, Nagasaki 852-8523, Japan. Tel.: +81 95 819 7838; fax: +81 95 819 7805.
E-mail address: okaneko@nagasaki-u.ac.jp (O. Kaneko).

1383-5769/$ – see front matter © 2008 Elsevier Ireland Ltd. All rights reserved.
doi:10.1016/j.parint.2008.09.005

Please cite this article as: Cao J, et al, Rhoptry neck protein RON2 forms a complex with microneme protein AMA1 in *Plasmodium falciparum* merozoites, Parasitol Int (2008), doi:10.1016/j.parint.2008.09.005

Plasmodium species in the late 1970s [3], but the molecular nature of its structure remains unresolved.

Recent studies in *Toxoplasma gondii* suggest that host cell invasion involves protein discharge from at least two apical secretory organelles, the micronemes and rhoptries, based on the observation that a microneme protein, Apical Membrane Protein 1 (AMA1), forms a complex with three rhoptry neck (RON) proteins: RON2, RON4 and Ts4705 (RON5) [4–6]. These proteins have predicted orthologs in *P. falciparum*, and the RON4 ortholog has been reported to associate with *Pf*AMA1 [7] and to be localized at the moving junction [8], suggesting that the complex (and likely its function) is conserved between *T. gondii* and *P. falciparum* [7]. Attempts to knock-out the AMA1 gene locus were unsuccessful in both *Plasmodium* [9] and *T. gondii* [10], and the conditional reduction of *Tg*AMA1 expression severely impaired the cell invasion ability of *T. gondii* [11], indicating AMA1 has an essential function. The conservation of the RON proteins among apicomplexan parasites suggest that their functions and protein interactions are also conserved in the biology of host cell invasion. However, in *Plasmodium*, the details of this complex have yet to be fully characterized. In this study, to better understand the moving junction complex formation in *Plasmodium*, we sought to characterize *Pf*RON2 and determine the nature of its interaction with *Pf*RON4 and *Pf*AMA1.

2. Materials and methods

2.1. Malaria parasites

P. falciparum cloned lines 3D7, HB3, Dd2, 7G8, FVO, and D10 were maintained *in vitro*, essentially as previously described [12].

2.2. DNA and RNA isolation

Genomic DNA (gDNA) was isolated from *P. falciparum* using IsoQuick™ (Orca Research Inc., Bothell, WA). To determine transcription levels throughout the asexual stages, schizonts were purified by differential centrifugation on a 70%/40% Percoll-sorbitol gradient, after which released merozoites were allowed to invade uninfected erythrocytes for 4 h before the clearance of all remaining schizonts using 5% D-sorbitol. Fractions of the culture were harvested immediately and 24 h later, and then at 6 h intervals thereafter. Total RNA was isolated from parasite-infected erythrocytes stored at −20 °C in RNA*later*™ (Qiagen, Valencia, CA), using the RNeasy Mini Kit (Qiagen). Following DNase treatment, complementary DNA (cDNA) was generated with random hexamers using an Omniscript Reverse Transcription Kit (Qiagen).

2.3. Polymerase chain reaction (PCR) amplification and sequencing

A TBLASTN search was performed against the *P. falciparum* genome database (3D7 parasite line) via PlasmoDB website (http://www.plasmodb.org/) [13] using the *Tg*RON2 amino acid sequence as a query. To evaluate the polymorphism of *Pf*RON2, five pairs of overlapping primers were used for PCR amplification from HB3, FVO, Dd2, D10, and 7G8 parasite lines, and sequences were determined by direct sequencing of the PCR-amplified DNA fragments using an ABI PRISM® 3100-*Avant* Genetic Analyzer (Applied Biosystems, Foster City, CA). Oligonucleotides used were as follows: fRON2.F2 (5′-GATTCCAATAATTATAATTCTGATAATG-3′) and fRON2.R2 (5′-CGTAAAATATTCATTATATGAAAGATATGC-3′), fRON2.F3 (5′-GCATTAGGAGAACTTGTTGAACCA-3′) and fRON2.R3 (5′-CATAATATCTAAATAGGTTTTTGCTGAC-3′), fRON2.F4 (5′-GGATTAGTATTTTTATATGCAATGATTG-3′) and fRON2.R4 (5′-GTTATTTTCTAATAAATGTTTACTATCTTC-3′), fRON2.F5 (5′-GATAAATGGGATCAATTTATAAATAAGG-3′) and fRON2.R5 (5′-GCTAGCTACTGGTCCTGCACCT-3′), and fRON2.F6 (5′-ATGCAATTACCTTACTTAAGTCAAATG-3′) and fRON2.R6 (5′-ATATAAAATGAAAATAACAGAAAAGGTTATG-3′).

2.4. Quantification of pfron2 transcripts

Transcription of *ron2* was evaluated in the HB3 parasite line by real-time reverse transcription (RT)-PCR using a QuantiTect SYBR Green PCR Kit (Qiagen) and a LightCycler System (Roche, Basel, Switzerland). As a control, transcription of *ama1* and *rhoph2* was also evaluated. Oligonucleotides used were as follows: fRON2.qF (5′-CAGAACTAAGCAAACATGTAAAACATG-3′) and fRON2.qR (5′-GTATAACGCCTTGCTCATTTCCTG-3′) for *pfron2* (product size is 133 bp); fAMA1.qF (5′-GGAAGAGGACAGAATTATTGGGAAC-3′) and fAMA1.qR (5′-CCTGAATCTTCTTGTTGGTATGTATG-3′) for *pfama1* (product size is 137 bp); fRhopH2.qF (5′-GTAACAACACTTACTAAGGCAGACT-3′) and fRhopH2.qR (5′-GTACAAAGCTACAATATTGTTAGATCT-3′) for *pfrhoph2* (product size is 210 bp). The same oligonucleotides were used to PCR-amplify DNA fragments to be ligated into the pGEM-T Easy® plasmid (Promega, Madison, WI) which was used to make a standard curve to evaluate the copy number of each transcript.

2.5. Antibodies

A DNA fragment encoding amino acid positions (aa) 21–98 of *Pf*RON2 was PCR-amplified from *P. falciparum* 3D7 gDNA and ligated into pEU-E01GST-N2, an expression plasmid with N-terminal glutathione S transferase (GST)-tag followed by a PreScission Protease cleavage site, designed specifically for the wheat germ cell-free protein expression system (CellFree Sciences Co., Ltd., Matsuyama, Japan) [14], to produce recombinant GST-fused fRON2N protein (GST-fRON2N). Oligonucleotides used in the PCR amplification were fRON2.SalF1 (5′-*GTCGAC*TCAGAACTAAGCAAACATGTAAAACATG-3′) and fRON2.SalR1 (5′-*GTCGAC*CCCATTATTCATTTCACTACCAGGA-3′) (SalI restriction sites are underlined). Produced GST-fRON2N was captured using a glutathione-Sepharose 4B column and eluted with 10 mM reduced gluthathione, pH 8.0. To generate anti-*Pf*RON2 sera, BALB/c mice were immunized subcutaneously with 20 μg of purified GST-fRON2N emulsified with Freund's adjuvant. A Japanese white rabbit was immunized subcutaneously with 500 μg of purified GST-fRON2N with Freund's adjuvant for the first time, followed by 250 μg thereafter. All immunizations were done 4 times at 3 week intervals, prior to collection of antisera. Rabbit anti-*Pf*RhopH2 serum was obtained from I. Ling (National Institute for Medical Research, UK) [15], Rabbit anti-*Pf*AMA1 serum was obtained from C. Long (National Institute of Health, USA), and mouse monoclonal anti-*Pf*RON4 antibody (Ab; 26C64F12) was obtained from J.-F. Dubremetz (Université de Montpellier 2, France) [7]. Rabbit anti-Clag3.1 serum was as previously described [16].

2.6. SDS-PAGE and Western blot analysis

The recombinant protein, GST-fRON2N, was digested with a PreScission Protease at 4 °C overnight before analysis. Triton X-100 extracts of *P. falciparum* or recombinant proteins were dissolved in SDS-PAGE loading buffer, incubated at 100 °C for 3 min, and subjected to electrophoresis under reducing conditions on a 5–20% polyacrylamide gel (ATTO, Japan). Proteins were then transferred to a 0.22 μm PVDF membrane (BioRad, Hercules, CA). The proteins were immunostained with antisera followed by horseradish peroxidase-conjugated secondary Ab (Biosource Int., Camarillo, CA) and visualized with Immobilon™ Western Chemiluminescent HRP Substrate (Millipore, Billerica, MA) on RX-U film (Fuji, Japan). The relative molecular sizes of the parasite-encoded proteins were calculated by reference to molecular size standards (BioRad).

2.7. Immunoprecipitation

Immunoprecipitation was carried out as previously described [17]. Briefly, proteins were extracted from late schizont parasite pellets by

Please cite this article as: Cao J, et al, Rhoptry neck protein RON2 forms a complex with microneme protein AMA1 in *Plasmodium falciparum* merozoites, Parasitol Int (2008), doi:10.1016/j.parint.2008.09.005

1% Triton X-100 treatment in phosphate-buffered saline (PBS) containing cOmplete Proteinase Inhibitor Cocktail Tablets (Roche). Supernatants (50 µl) were pre-incubated at 4 °C for 1 h with 20 µl of 50% protein G-conjugated beads (GammaBind Plus Sepharose; GE Healthcare) in NETT buffer (50 mM Tris–HCl, 0.15 M NaCl, 1 mM EDTA, and 0.5% Triton X-100) supplemented with 0.5% BSA (fraction V; Sigma-Aldrich). Recovered supernatants were incubated with rabbit antisera (anti-*Pf*RON2, anti-*Pf*AMA1, or anti-*Pf*RhopH2) or mouse anti-*Pf*RON4 Ab with gentle rotation at 4 °C for 2 h and then 20 µl of 50% protein G-conjugated beads were added. After 1 h incubation at 4 °C, the beads were washed once with NETT-0.5% BSA, once with NETT, once with high-salt NETT (0.5 M NaCl), once with NETT, and once with low-salt NETT (0.05 M NaCl and 0.17% Triton X-100). Finally, proteins were extracted from the protein G-conjugated beads by incubation with SDS-PAGE reducing loading buffer at 100 °C for 3 min. Supernatants were collected for Western blot analysis.

2.8. Indirect immunofluorescence assay

Thin smears of schizont-enriched *P. falciparum*-infected erythrocytes (Dd2 parasite line) were prepared on glass slides and stored at −80 °C. The smears were thawed, formaldehyde-fixed, and preincubated with PBS containing 5% non-fat milk at 37 °C for 30 min. They were then incubated with antisera at 37 °C for 1 h, followed by fluorescein isothiocyanate (FITC)-conjugated goat anti-(IgG and IgM) secondary Ab (Jackson ImmunoResearch Laboratories, West Grove, PA) and Alexa546-conjugated goat anti-(IgG and IgM) secondary Ab (Invitrogen, Carlsbad, CA) at 37 °C for 30 min. Nuclei were stained with 4′,6-diamidino-2-phenylindole (DAPI). Slides were mounted in ProLong Gold antifade reagent (Invitrogen) and viewed under oil-immersion. High resolution image-capture and processing were performed using a confocal scanning laser microscope (LSM5 PASCAL; Carl Zeiss MicroImaging, Thornwood, NY). Images were processed in Adobe Photoshop (Adobe Systems Inc., San José, CA).

2.9. Immunoelectron microscopy

Parasites were fixed for 15 min on ice in a mixture of 1% paraformaldehyde–0.1% glutaraldehyde in 0.1 M phosphate buffer (pH 7.4). Fixed specimens were washed, dehydrated, and embedded in LR White resin (Polysciences, Inc., Warrington, PA) as previously described [18,19]. Thin sections were blocked at 37 °C for 30 min in PBS containing 5% non-fat milk and 0.01% Tween 20 (PBS-MT). Grids were then incubated at 4 °C overnight with mouse anti-*Pf*RON2 or control sera in PBS-MT. After washing with PBS containing 10% BlockAce (Yukijirushi, Sapporo, Japan) and 0.01% Tween 20 (PBS-BT), the grids were incubated at 37 °C for 1 h with goat anti-mouse IgG conjugated to 10 nm gold particles (Amersham Life Science, Arlington, IL) diluted 1:20 in PBS-MT, rinsed with PBS-BT, and fixed on ice for 10 min in 2.5% glutaraldehyde to stabilize the gold. Then the grids were rinsed with distilled water, dried, and stained with uranyl acetate and lead citrate. Samples were examined with a transmission electron microscope (JEM-1230; JEOL Ltd., Tokyo, Japan).

2.10. Primary structure analysis of the protein

Signal peptide sequence was evaluated by SignalP3.0 [20]. Transmembrane region was evaluated by TMpred [21] and TMHMM2.0 [22]. Low complexity region was evaluated by Globplot 2.3 [23]. Amino acid sequence alignment was generated by MUSCLE [24].

2.11. Statistical analysis

Number of nonsynonymous substitutions over numbers of nonsynonymous sites (d_N), number of synonymous substitutions over numbers of synonymous sites (d_S), and their standard errors were computed using the Nei-Gojobori method with Jukes-Cantor correction implemented in MEGA 4.0.1 [25]. Standard errors were estimated using the bootstrap method with 500 replications. The statistical difference between d_N and d_S was tested using a one-tail *Z*-test with 500 bootstrap pseudosamples.

3. Results

3.1. RON2 orthologs of apicomplexan parasites

Using *Tg*RON2 as a query in BLAST analyses [26], and similar analyses using the predicted orthologs thus identified, we found RON2 orthologs in *P. falciparum* (*Pf*RON2; PF14_0495, PlasmoDB), *P. yoelii* 17XNL strain (*Py*RON2; PY06813, TIGR), *P. knowlesi* H strain (*Pk*RON2; PKH_125430 or PK14_2335w, Sanger Centre), and *P. vivax* Sal-I strain (*Pv*RON2; Pv117880, TIGR), *P. berghei* (*Pb*RON2; Contig5108), *P. chabaudi* (*Pch*RON2; Contig882.0), *Theileria annulata* (*Ta*RON2; Fig. S1A, TA19445 and TA19390, Sanger Centre [27]), *Theileria parva* (*Tp*RON2; Fig. S1B, TP01_0014, TIGR [28]), and *Babesia bigemina* (*Bbig*RON2; Fig. S1C, Contig3449, Sanger Centre). The RON2 were fragmented in the *P. berghei*, *P. chabaudi*, *T. annulata*, and *T. parva* genome nucleotide sequence databases, and full-length versions were constructed (supplementary Table S1).

3.2. PfRON2 protein structure and similarity to RhopH1/Clag proteins

The full-length *Pf*RON2 protein consists of 2189 residues with a putative signal peptide sequence at its N-terminus from amino acid positions (aa) 1 to 20. An interspecies variable region (aa 55–878), exhibiting low complexity and many repeats [23], was identified by comparing 6 *Plasmodium* RON2 amino acid sequences (Figs. 1 and S2). A BLASTP search using the conserved region of *Pf*RON2 (aa 879–2189) as a query identified *P. vivax* RhopH1/Clag homolog (XP_001616939.1, aa 251–394; E = 0.001) as possessing homology with *Pf*RON2 aa 1105–1259. A Position-Specific Iterated BLAST search using *Pf*RON2 aa 1105–1259 as a query converged at iteration 3 and indentified most of the RhopH1/Clag genes in *Plasmodium* species. Alignment of RhopH1/Clag with RON2 from multiple genera identifies a predicted globular domain that is likely stabilized by disulfide bonds between 4 conserved Cys residues (Fig. 2). Three transmembrane regions were predicted by TMpred, however TMHMM2.0 predicted only a single transmembrane region for all *Plasmodium* RON2 orthologs assessed.. Interestingly, TMpred predicted a putative transmembrane region in the region conserved between RhopH1/Clag and RON2 (Fig. 2). Because RhopH1/Clag is a component of a soluble protein complex, we considered that these predicted transmembrane regions in RhopH1/Clag and RON2 constitute a likely hydrophobic region buried within a globular domain. Another predicted transmembrane region at aa 1114–1133 in *Pf*RON2 is also possibly hydrophobic region buried within a globular domain. TMpred considers the observation that there is an overrepresentation of positively charged amino acid

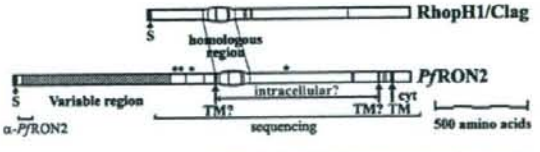

Fig. 1. Schematic representation of *Pf*RON2. S and TM indicate putative signal peptide (aa 1–20) and transmembrane sequences, respectively. The shaded box indicates an interspecies variable region. Vertical red bars indicate conserved Cys residues among orthologous sequences. Homologous region between RhopH1/Clag and RON2 is indicated by a yellow box. The region used to generate anti-*Pf*RON2 sera (α-*Pf*RON2) and the region sequenced in the laboratory lines (sequencing) are indicated. Asterisks indicate polymorphic sites.

Please cite this article as: Cao J, et al, Rhoptry neck protein RON2 forms a complex with microneme protein AMA1 in *Plasmodium falciparum* merozoites, Parasitol Int (2008), doi:10.1016/j.parint.2008.09.005

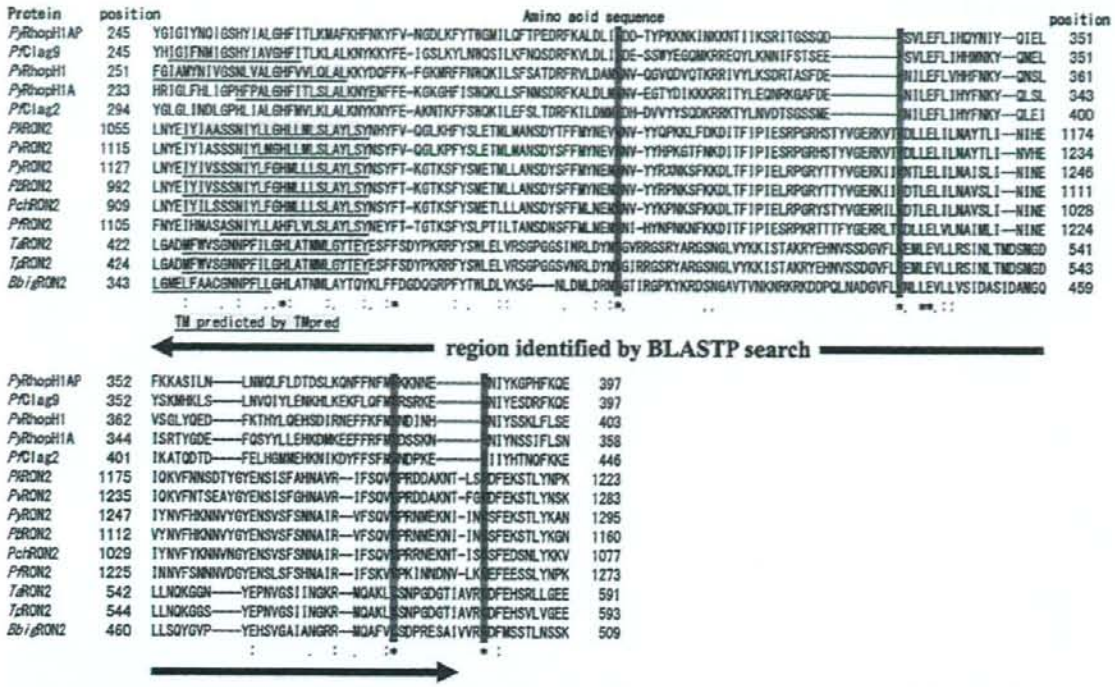

Fig. 2. Amino acid alignment of *Plasmodium* RON2 and RhopH1/Clag. Alignment was generated by MUSCLE [24] with manual correction. "*" indicates that the residues in that column are identical in all sequences in the alignment. ":" indicates conserved substitutions and "." indicates semi-conserved substitutions. In addition to 9 RON2 sequences, *P. falciparum* Clag2 (AAC71977), Clag9 (CAD52032), *P. yoelii* RhopH1A (BAB70675), RhopH1AP (BAB70677), and *Pv*RhopH1 (contig 1047) were used to generate the alignment. Cys residues are highlighted in red. The region possessing homology between RhopH1/Clag and RON2 as identified by BLASTP is indicated by the bar under the alignment.

residues in the cytoplasmic loops of the transmembrane protein [21], which is a likely explanation for this discrepancy.

3.3. *PfRON2 transcription peaks at the schizont stage*

To determine the transcription pattern in the asexual stages of the parasite life-cycle, quantitative RT-PCR was performed on the HB3 parasite line prepared from a synchronized culture harvested at 6 h intervals. Both RON2 and AMA1 transcriptions were seen to peak around 36–40 h after invasion, when parasites were in the schizont stage. AMA1 showed a broader and flatter transcription peak than RON2 (Fig. 3). Transcriptome data compiled in the PlasmoDB website [13,29] also indicated a milder wave crest of AMA1 transcripts compared with RON2.

3.4. *Complex formation of PfRON2, PfRON4, and PfAMA1*

Mouse and rabbit anti-*Pf*RON2 sera were generated using recombinant GST-fRON2N. Firstly, we evaluated the reactivity of anti-*Pf*RON2 sera by Western blot using recombinant proteins. Both antisera recognized the fRON2N component of the recombinant protein after cleavage (Fig. S3, filled arrows). Cleaved 26.4-kDa GST component (Fig. S3, arrowheads) and 46-kDa GST-fused PreScission protease (Fig. S3, unfilled arrow) were also recognized by these Abs.

Secondly, we evaluated the reactivity of these sera against native RON2 proteins extracted from schizont stage *P. falciparum* (HB3 line) by Western blot analysis. Both antisera reacted with a band slightly larger than 250 kDa (Fig. 4A, arrows), which is similar to the predicted molecular weight of *Pf*RON2 after exclusion of the putative signal peptide sequence (247 kDa). An 80-kDa band was detected by both mouse and rabbit antisera in HB3 extract, for which the exact identity is not known, but a possible processed product of *Pf*RON2. A 55-kDa band detected with rabbit antiserum was also detected with preimmune serum, suggesting that this band was unrelated to

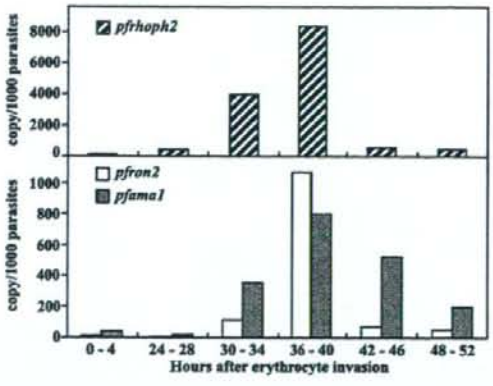

Fig. 3. Transcriptional analysis by quantitative RT-PCR of *pfrhoph2*, *pfron2*, and *pfama1* genes during blood stages of *P. falciparum* (HB3 line). *Y*-axis indicates copy number of each transcript detected per 1000 parasites. Similar results were observed in 3 independent experiments (data not shown).

Please cite this article as: Cao J, et al. Rhoptry neck protein RON2 forms a complex with microneme protein AMA1 in *Plasmodium falciparum* merozoites. Parasitol Int (2008), doi:10.1016/j.parint.2008.09.005

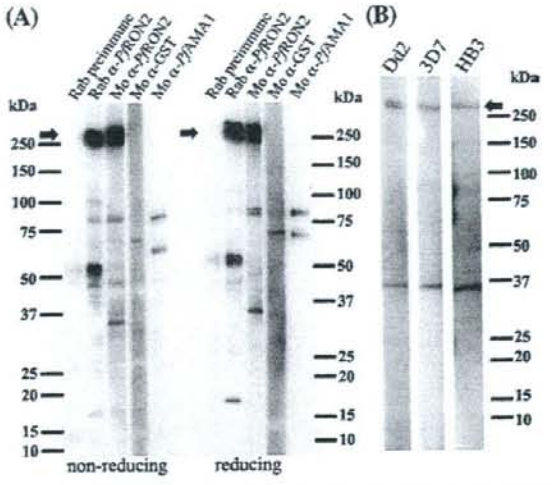

Fig. 4. Western blot analysis of antisera against native parasite proteins. (A) Schizont-enriched parasite extracts were stained by rabbit preimmune serum, (Rab preimmune), rabbit anti-*Pf*RON2 (Rab α-*Pf*RON2), mouse anti-fRON2N (Mo α-*Pf*RON2), and Abs against GST (Mo α-GST) or *Pf*AMA1 (Mo α-*Pf*AMA1) under both reducing and non-reducing conditions. Both mouse and rabbit anti-*Pf*RON2 sera detected a band slightly larger than 250 kDa. (B) Western blot of schizont-enriched parasite extracts from 3 different *P. falciparum* lines, Dd2, 3D7, and HB3 with mouse anti-fRON2N serum. Arrows indicate predicted *Pf*RON2 bands.

*Pf*RON2. A 35-kDa band was detected with mouse antiserum but not with rabbit antiserum, suggesting that it is also unrelated to RON2.

To evaluate the interaction between *Pf*RON2, *Pf*RON4, and *Pf*AMA1, we performed immunoblotting against immunoprecipitated materials from mature schizont-rich parasite extracts (Fig. 5). We found that RON2 was detected in the precipitated fraction using anti-*Pf*AMA1 or anti-*Pf*RON4. In the reciprocal experiment, *Pf*AMA1 and *Pf*RON4 were also detected in the precipitated fraction of anti-*Pf*RON2 serum. Although it is theoretically possible that such immunoprecipitated fractions contained the *Pf*RON2-*Pf*RON4, *Pf*RON2-*Pf*AMA1, and *Pf*RON4-*Pf*AMA1 dimeric complexes as appropriate to the primary antibody, considering that these 3 proteins are distinct molecules that do not possess any similarity each other, this specific co-immunoprecipitation suggests complex formation among *Pf*RON2, *Pf*RON4, and *Pf*AMA1 in *P. falciparum*. The fact that both the 83-kDa proform and the 66-kDa processed form were co-precipitated with *Pf*RON2 indicated that a region responsible for complex formation was located in the 66-kDa form of AMA1 [30]. Neither of these was detected in the anti-RhopH2 immunoprecipitate, thereby excluding not only the possibility of *Pf*RON2 involvement in the RhopH complex, but also potential carryover due to insufficient or inadequate washing steps.

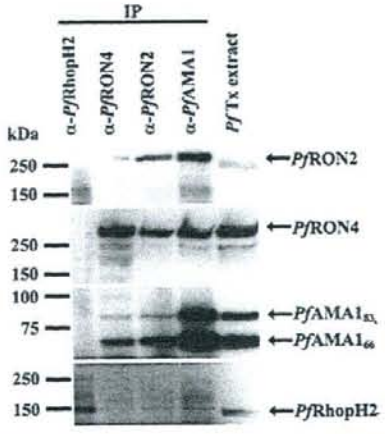

Fig. 5. *Pf*RON2 is co-precipitated with *Pf*RON4 and *Pf*AMA1. Schizont-rich parasite Triton X-100 extracts (*Pf* Tx extract) were immunoprecipitated (IP) with rabbit sera against *Pf*RhopH2 (α-*Pf*RhopH2), *Pf*RON2 (α-*Pf*RON2), *Pf*AMA1 (α-*Pf*AMA1) or mouse monoclonal Ab against *Pf*RON4 (α-*Pf*RON4), then stained against *Pf*RON2, *Pf*AMA1, *Pf*RON4, or *Pf*RhopH2. $AMA1_{83}$ is a proprotein form and $AMA1_{66}$ is a processed form.

3.5. RON2 is expressed at the rhoptry neck of Plasmodium merozoites

Dual labeling indirect immunofluorescent assay was performed using anti-*Pf*RON2 with either anti-*Pf*AMA1 (microneme marker), anti-Clag3.1 (rhoptry body marker), or anti-*Pf*RON4 (rhoptry neck marker) antibodies in order to determine the sub-cellular location of *Pf*RON2 in *P. falciparum* (Fig. 6). In segmented schizonts, RON2 antisera produced a punctate pattern of fluorescence and each developing merozoite showed a single small punctate *Pf*RON2-positive signal located at the apical end. Although some parts of the *Pf*RON2 signal

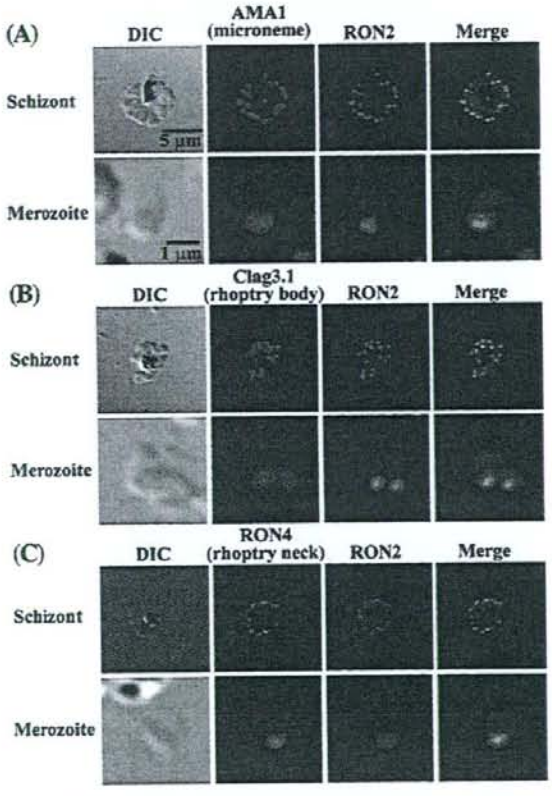

Fig. 6. *Pf*RON2 is expressed at the apical end of *Plasmodium* merozoites. Schizont-infected erythrocytes and merozoites were dual-labeled with antisera against *Pf*RON2 and *Pf*AMA1 (A), *Pf*Clag3.1 (B), or *Pf*RON4 (C). Merged images are shown in the right panels. All segmented schizonts and merozoites are positive for *Pf*RON2. Nuclei are counterstained with DAPI. Colocalization of *Pf*RON2 with *Pf*RON4 (rhoptry neck marker) was observed but neither colocalized with *Pf*Clag3.1 (rhoptry body marker) nor *Pf*AMA1 (microneme marker). To eliminate the background staining, negative control sera were always used and images were assessed (data not shown).

Please cite this article as: Cao J, et al. Rhoptry neck protein RON2 forms a complex with microneme protein AMA1 in *Plasmodium falciparum* merozoites. Parasitol Int (2008), doi:10.1016/j.parint.2008.09.005

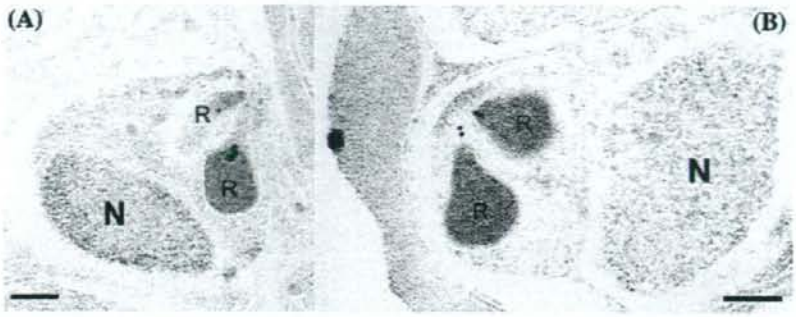

Fig. 7. Rhoptry neck localization of *Pf*RON2 by immunoelectron microscopy. Longitudinally sectioned merozoites in schizont-infected erythrocytes were labeled with anti-*Pf*RON2 serum followed by secondary Ab conjugated with gold particles. Gold particles were restricted to the narrow neck portion of the rhoptries (R). Two different images are shown (A and B). N indicates nucleus. Bars = 200 nm.

overlapped with microneme protein AMA1 and rhoptry body protein Clag3.1, it did not colocalize well with those markers, whereas complete colocalization was observed with the rhoptry neck marker *Pf*RON4.

Immunoelectron microscopy was carried out to determine the precise localization of the protein. *Pf*RON2 was detected in the neck portion of the pear-shaped rhoptries in segmented schizonts (Fig. 7). Thus *Pf*RON2 is seen to compartmentalize in the rhoptry neck.

3.6. Potential positive diversifying selection on *PfRON2*

To evaluate the polymorphic nature of *Pf*RON2, we sequenced the *pfron2* nucleotide sequence (2459–6570), excluding the 5′ low complexity region, in 5 *P. falciparum* parasite lines and compared them with the sequence from the genome database (3D7 line). A total of 5 nonsynonymous nucleotide substitutions were observed at nucleotide positions 2615, 2710, 2914, 4391 and 4392, resulting 4 amino acid substitutions (Table 1). An excess of nonsynonymous substitutions ($d_N = 0.0007 \pm 0.0003$) over synonymous substitutions ($d_S = 0.0002 \pm 0.0002$) was detected ($P = 0.0333$), indicating *Pf*RON2 is subject to positive diversifying selection.

4. Discussion

In this study, we characterized *P. falciparum* RON2 for its protein structure, transcription profiles, intracellular localization, and complex formation with *Pf*RON4 and *Pf*AMA1.

*Pf*RON2 possesses a region harboring homology with another rhoptry protein RhopH1/Clag, a component of the RhopH complex that possesses erythrocyte binding ability [16,31,32]. Co-immunoprecipitation showed that *Pf*RON2 does not form a complex with RhopH2, suggesting that *Pf*RON2 is unlikely to be a component of the RhopH complex. Because RON2 orthologs can be found in other apicomplexan parasites and RhopH1/Clag is found only in *Plasmodium* species, RhopH1/Clag probably evolved via acquisition of a conserved functional domain from RON2 during its generation in *Plasmodium* species. Thus, this homologous region may have a common function between these two complexes. The sequence of *Tg*RON2 deposited to the database (GenBank accession number DQ096563) only possesses the C-terminal half of the conserved region between RON2 and RhopH1/Clag. By comparing *Tg*RON2 gDNA and cDNA sequences, we noticed that intron 3 is relatively large (2272 bp) and contains a potential sequence encoding the N-terminal portion of the conserved region. Thus it is possible that there is another alternatively spliced transcript encoding the full length of the conserved region. Alternatively, it is also possible that this region represents an ancient vestigial exon.

Interestingly, we could readily detect complex formation between AMA1 and RON proteins in the extract obtained from mature schizont-rich parasites, suggesting that complex formation had already occurred at the schizont stage likely at the apical end upon secretion of RON proteins from rhoptry and AMA1 from microneme. This is in contrast to the other apicomplexa parasite *T. gondii*, in which the AMA1-RON complex was proposed to form at the initial contact with the host cell. The precise timing of the complex formation is not clear, but may vary depending on the parasite species. Among RON proteins characterized thus far, only *Tg*RON4 was visualized to locate at the moving junction during cell invasion. Whether *Pf*RON2 and *Pf*RON4 locate at the moving junction and whether the complex remains intact during cell invasion are still need to be clarified. We found that *Pf*RON2 degraded more rapidly than *Pf*RON4 after extraction (Fig. S4), which may explain the previous observation by Alexander et al. (2006), who did not detect *Pf*RON2 in the immunoprecipitant with anti-*Pf*AMA1 Ab [7].

The association between the 83-kDa proform of *Pf*AMA1 with RON proteins raises the possibility that the processing of *Pf*AMA1 from the 83-kDa form to 66-kDa form occurs not only in the microneme, as previously proposed [33], but also on the apical tip of the merozoite after release from the microneme in mature schizonts. If this is the case, it is not clear whether this AMA1 processing occurs after complex formation with RON proteins or is mainly achieved prior to this. However, it is formally possible that disruption of the different intracellular microorganelles during the experimental procedure resulted in an artificial complex formation of *Pf*AMA1 proform, for which further studies are required.

Due to the fact that *P. falciparum* AMA1 exhibits relatively high polymorphism between lines, which is considered to be generated by positive diversifying selection under the human immune pressure, we evaluated the polymorphic nature of *Pf*RON2. Although the level of polymorphism of RON2 is not high, the fact that $d_N > d_S$ suggests that positive diversifying selection does indeed act on RON2. Three types of

Table 1
Nucleotide and amino acid polymorphism of *Pf*RON2

Nucleotide positions (amino acid) [a]	Parasite line					
	3D7	7G8	HB3	Dd2	FVO	D10
2614–2616	tCa (Ser)	tCa (Ser)	tCa (Ser)	tCa (Ser)	tCa (Ser)	tTa (Leu)
2710–2712	Cat (His)	Cat (His)	Cat (His)	Tat (Tyr)	Tat (Tyr)	Tat (Tyr)
2914–2916	Gac (Asp)	Gac (Asp)	Cac (His)	Gac (Asp)	Gac (Asp)	Gac (Asp)
4390–4392	gAA (Glu)	gAA (Glu)	gAC (Asp)	gGC (Gly)	gGC (Gly)	gAA (Glu)

[a] Nucleotide numbering is after the 3D7 line sequence.

Please cite this article as: Cao J, et al, Rhoptry neck protein RON2 forms a complex with microneme protein AMA1 in *Plasmodium falciparum* merozoites, Parasitol Int (2008), doi:10.1016/j.parint.2008.09.005

amino acid substitutions found at aa 1464 (Asp, Glu, and Gly) suggests that this particular site is under diversifying selection and is possibly to be exposed to host immunity. Thus, *Pf*RON2 not only appears to have an important role in host cell invasion by apicomplexan parasites, but also is a potential target for malaria intervention strategies.

Acknowledgements

We thank N Iyoku for her expertise, I Ling for anti-*Pf*RhopH2 serum, C Long for anti-*Pf*AMA1 serum, anti-*Pf*RON4 antibody (26C64F12) for J-F Dubremetz, and R Culleton for critical reading. Preliminary sequence data of *P. knowlesi*, *P. berghei*, *P. chabaudi*, and *B. bigemina* were produced by the corresponding groups at the Sanger Institute website at http://www.sanger.ac.uk/. Preliminary sequence data of *P. vivax* was produced at the Institute for Genomic Research website at http://www.tigr.org. This work was supported in part by Grants-in-Aid for Scientific Research 17590372 and 17406009 (to OK) from the Ministry of Education, Culture, Sports, Science and Technology, Japan. JC acknowledges the support of National Natural Science Foundation of China 30700695.

Appendix A. Supplementary data

Supplementary data associated with this article can be found, in the online version, at doi:10.1016/j.parint.2008.09.005.

References

[1] Snow RW, Guerra CA, Noor AM, Myint HY, Hay SI. The global distribution of clinical episodes of *Plasmodium falciparum* malaria. Nature 2005;434:214–7.
[2] Kaneko O. Erythrocyte invasion: vocabulary and grammar of the *Plasmodium* rhoptry. Parasitol Int 2007;56:255–62.
[3] Aikawa M, Miller LH, Johnson J, Rabbege J. Erythrocyte entry by malarial parasites. a moving junction between erythrocyte and parasite. J Cell Biol 1978;77:72–82.
[4] Boothroyd JC, Dubremetz JF. Kiss and spit: the dual roles of *Toxoplasma* rhoptries. Nat Rev Microbiol 2008;6:79–88.
[5] Alexander DL, Mital J, Ward GE, Bradley P, Boothroyd JC. Identification of the moving junction complex of *Toxoplasma gondii*: a collaboration between distinct secretory organelles. PLoS Pathog 2005;1:e17.
[6] Lebrun M, Michelin A, El Hajj H, Poncet J, Bradley PJ, Vial H, et al. The rhoptry neck protein RON4 re-localizes at the moving junction during *Toxoplasma gondii* invasion. Cell Microbiol 2005;7: 1823–33.
[7] Alexander DL, Arastu-Kapur S, Dubremetz JF, Boothroyd JC. *Plasmodium falciparum* AMA1 binds a rhoptry neck protein homologous to TgRON4, a component of the moving junction in *Toxoplasma gondii*. Eukaryot Cell 2006;5:1169–73.
[8] Baum J, Tonkin CJ, Paul AS, Rug M, Smith BJ, Gould SB, et al. A malaria parasite formin regulates actin polymerization and localizes to the parasite-erythrocyte moving junction during invasion. Cell Host Microbe 2008;3:188–98.
[9] Triglia T, Healer J, Caruana SR, Hodder AN, Anders RF, Crabb BS, et al. Apical membrane antigen 1 plays a central role in erythrocyte invasion by *Plasmodium* species. Mol Microbiol 2000;38:706–18.
[10] Hehl AB, Lekutis C, Grigg ME, Bradley PJ, Dubremetz JF, Ortega-Barria E, et al. *Toxoplasma gondii* homologue of *Plasmodium* apical membrane antigen 1 is involved in invasion of host cells. Infect Immun 2000;68:7078–86.
[11] Mital J, Meissner M, Soldati D, Ward GE. Conditional expression of *Toxoplasma gondii* apical membrane antigen-1 (TgAMA1) demonstrates that TgAMA1 plays a critical role in host cell invasion. Mol Biol Cell 2005;16:4341–9.
[12] Trager W, Jensen JB. Human malaria parasites in continuous culture. Science 1976;193:673–5.
[13] Bahl A, Brunk B, Crabtree J, Fraunholz MJ, Gajria B, Grant GR, et al. PlasmoDB: the *Plasmodium* genome resource. a database integrating experimental and computational data. Nucleic Acids Res 2003;31:212–5.
[14] Tsuboi T, Takeo S, Iriko H, Jin L, Tsuchimochi M, Matsuda S, et al. The wheat germ cell-free based production of malaria proteins for discovery of novel vaccine candidates. Infect Immun 2008;76:1702–8.
[15] Ling IT, Kaneko O, Narum DL, Tsuboi T, Howell S, Taylor HM, et al. Characterisation of the *rhoph2* gene of *Plasmodium falciparum* and *Plasmodium yoelii*. Mol Biochem Parasitol 2003;127:47–57.
[16] Kaneko O, Yim Lim BY, Iriko H, Ling IT, Otsuki H, Grainger M, et al. Apical expression of three RhopH1/Clag proteins as components of the *Plasmodium falciparum* RhopH complex. Mol Biochem Parasitol 2005;143:20–8.
[17] Kaneko O, Fidock DA, Schwartz OM, Miller LH. Disruption of the C-terminal region of EBA-175 in the Dd2/Nm clone of *Plasmodium falciparum* does not affect erythrocyte invasion. Mol Biochem Parasitol 2000;110:135–46.
[18] Torii M, Adams JH, Miller LH, Aikawa M. Release of merozoite dense granules during erythrocyte invasion by *Plasmodium knowlesi*. Infect Immun 1989;57: 3230–3.
[19] Aikawa M, Atkinson CT. Immunoelectron microscopy of parasites. Adv Parasitol 1990;29:151–214.
[20] Bendtsen JD, Nielsen H, von Heijne G, Brunak S. Improved prediction of signal peptides: signalP 3.0. J Mol Biol 2004;340:783–95.
[21] Hofmann K, Stoffel W. TMbase – a database of membrane spanning proteins segments. Biol Chem Hoppe-Seyler 1993;374:166.
[22] Krogh A, Larsson B, von Heijne G, Sonnhammer EL. Predicting transmembrane protein topology with a hidden Markov model: application to complete genomes. J Mol Biol 2001;305:567–80.
[23] Linding R, Russell RB, Neduva V, Gibson TJ. GlobPlot: exploring protein sequences for globularity and disorder. Nucleic Acids Res 2003;31:3701–8.
[24] Edgar RC. MUSCLE: multiple sequence alignment with high accuracy and high throughput. Nucleic Acids Res 2004;32:1792–7.
[25] Tamura K, Dudley J, Nei M, Kumar S. MEGA4: Molecular Evolutionary Genetics Analysis (MEGA) software version 4.0. Mol Biol Evol 2007;24:1596–9.
[26] Altschul SF, Madden TL, Schäffer AA, Zhang J, Zhang Z, Miller W, et al. Gapped BLAST and PSI-BLAST: a new generation of protein database search programs. Nucleic Acids Res 1997;25: 3389–402.
[27] Pain A, Renauld H, Berriman M, Murphy L, Yeats CA, Weir W, et al. Genome of the host-cell transforming parasite *Theileria annulata* compared with *T. parva*. Science 2005;309:131–3.
[28] Gardner MJ, Bishop R, Shah T, de Villiers EP, Carlton JM, Hall N, et al. Genome sequence of *Theileria parva*, a bovine pathogen that transforms lymphocytes. Science 2005;309:134–7.
[29] Le Roch KG, Zhou Y, Blair PL, Grainger M, Moch JK, Haynes JD, et al. Discovery of gene function by expression profiling of the malaria parasite life cycle. Science 2003;301:1503–8.
[30] Howell SA, Withers-Martinez C, Kocken CH, Thomas AW, Blackman MJ. Proteolytic processing and primary structure of *Plasmodium falciparum* apical membrane antigen-1. J Biol Chem 2001;276:31311–20.
[31] Ghoneim A, Kaneko O, Tsuboi T, Torii M. The *Plasmodium falciparum* RhopH2 promoter and first 24 amino acids are sufficient to target proteins to the rhoptries. Parasitol Int 2007;56:31–43.
[32] Rungruang T, Kaneko O, Murakami Y, Tsuboi T, Hamamoto H, Akimitsu N, et al. Erythrocyte surface glycosylphosphatidyl inositol anchored receptor for the malaria parasite. Mol Biochem Parasitol 2005;140:13–21.
[33] Healer J, Triglia T, Hodder AN, Gemmill AW, Cowman AF. Functional analysis of *Plasmodium falciparum* apical membrane antigen 1 utilizing interspecies domains. Infect Immun 2005;73:2444–51.

Please cite this article as: Cao J, et al. Rhoptry neck protein RON2 forms a complex with microneme protein AMA1 in *Plasmodium falciparum* merozoites. Parasitol Int (2008), doi:10.1016/j.parint.2008.09.005

Malaria Journal

BioMed Central

Research

Open Access

SURFIN$_{4.1}$, a schizont-merozoite associated protein in the SURFIN family of *Plasmodium falciparum*

Fingani A Mphande[1], Ulf Ribacke[1], Osamu Kaneko[2], Fred Kironde[3], Gerhard Winter[1,4] and Mats Wahlgren*[1]

Address: [1]Department of Microbiology, Tumor and Cell Biology (MTC) Karolinska Institutet and Swedish Institute for Infectious Disease Control, Nobel's väg 16, Box 280, SE-171 77, Stockholm, Sweden, [2]Department of Protozoology, Institute of Tropical Medicine, Nagasaki University, 1-12-4 Sakamoto, Nagasaki 852-8523, Japan, [3]Department of Biochemistry, Makerere University, Kampala, Uganda and [4]Department of General Practice, Flinders University, Adelaide, Australia

Email: Fingani A Mphande - fingani.mphande@smi.se; Ulf Ribacke - ulf.ribacke@smi.se; Osamu Kaneko - okaneko@nagasaki-u.ac.jp; Fred Kironde - kironde@starcom.co.ug; Gerhard Winter - gerd.winter@eliott-winter.com; Mats Wahlgren* - mats.wahlgren@ki.se

* Corresponding author

Published: 1 July 2008

Malaria Journal 2008, **7**:116 doi:10.1186/1475-2875-7-116

Received: 12 November 2007

Accepted: 1 July 2008

This article is available from: http://www.malariajournal.com/content/7/1/116

Abstract

Background: In its effort to survive the human immune system, *Plasmodium falciparum* uses several parasite-derived antigens most of which are expressed at the surface of the parasitized red blood cells (pRBCs). Recently SURFINs, a new family of antigens encoded by the *surf* multi-gene family, has been reported. One member of the family, SURFIN$_{4.2}$, was found present both at the pRBC-surface and at the merozoite apex.

Methods: The presence of a second SURFIN member, SURFIN$_{4.1}$ (PFD0100c, PFD0105c) is reported here. Bioinformatic tools were used to study the structure of the *surf*$_{4.1}$ gene. To investigate the expression of *surf* genes PCR and real-time quantitative PCR (Rt-QPCR) were employed and Northern and Western blots were used to confirm the size of the *surf*$_{4.1}$ gene and the SURFIN$_{4.1}$ protein respectively. Localization of SURFIN$_{4.1}$ was determined using immunofluorescence assays.

Results: The *surf*$_{4.1}$ gene was found present in one copy by Rt-QPCR in some parasites (3D7AH1, 3D7S8, 7G8) whereas six copies of the gene were identified in FCR3 and FCR3S1.2. *surf*$_{4.1}$ was found transcribed in the late asexual stages of the parasite beginning ≈32 hours post invasion and throughout the schizont stages with the level of transcription peaking at late schizogony. The levels of transcript correlated with the number of gene copies in FCR3 and 3D7S8. *surf*$_{4.1}$ was found to encode a polypeptide of ≈Mw 258 kDa (SURFIN$_{4.1}$) present within the parasitophorous vacuole (PV), around free merozoites as merozoite-associated material, but not at the pRBC-surface. Despite multiple *surf*$_{4.1}$ gene copies in some parasites this was not reflected in the levels of SURFIN$_{4.1}$ polypeptide.

Conclusion: SURFIN$_{4.1}$ is a member of the SURFINs, present in the PV and on the released merozoite. The results suggest different SURFINs to be expressed at different locations in the parasite and at distinct time-points during the intra-erythrocytic cycle.

Background

The erythrocytic life cycle of *Plasmodium falciparum* is characterized by complex interactions of parasite derived surface exposed antigens with host receptors and immune defence proteins. At the surface of the the parasitized red blood cells (pRBCs), parasite antigens provide adhesive properties and at the same time allow for limited parasite resistance to the host immune response by virtue of great sequence variability. In case of the well-characterized surface antigen *Plasmodium falciparum* erythrocyte membrane protein 1 (PfEMP1), a multi-adhesive variable ligand of 200–400 kDa, this is achieved by clonal exchange, "switching" of the mutually expressed PfEMP1 encoding *var* gene. A unique set of ≈60 *var* genes is present in each parasite genome [1-3]. With the release of merozoites from the host cell, a number of additional parasite proteins are exposed to the immune system, which, in response to the host immune pressure, show polymorphisms or are differentially expressed [4].

The merozoite, which is the invasive form of *P. falciparum*, invades erythrocytes in a cascade of events in which multiple receptor-ligand interactions facilitate parasite attachment, reorientation, junction formation and entry [5-9]. The machinery employed in this process is complex and involves proteins at the merozoite surface and in specialized secretory organelles at the merozoite apex [10]. Triggered by the initial parasite attachment to the host cell, micronemes and/or rhoptries release their contents. The Duffy binding-like (DBL) family (EBA-175 and its paralogues EBA-140 (BAEBL) and EBA-181 (JESEBL) [11,12]) in micronemes and the reticulocyte binding like (RBL) family (PfRh1, PfRh2a, PfRh2b, PfRh3 and PfRh4 [13-16]) in the neck of rhoptries have been shown to be relevant for merozoite infectivity [4]. In *P. falciparum*, several copies of Pf *Rh1* gene were reported in FCR3, W2mef, and FCB1 (13, 3 and 4 respectively) when compared to 3D7. Thus, apart from the different protein antigens expressed on the surface of the merozoite, the complexity of the malaria parasite is increasing by the introduction of gene duplications and deletions [17-19].

SURFINs are a small family of large (200–300 kDa) proteins, which are composed of domains structurally related to PvSTP1 of *Plasmodium vivax* but also other exported and surface exposed parasite proteins [20], including PfEMP1, the *P. vivax* VIR family and *Plasmodium knowlesi* variant surface antigen (SICA*var*). In accordance with this structural relationship, $SURFIN_{4.2}$ was found co-transported with PfEMP1 to the pRBC-surface. The protein is also observed on the merozoite as merozoite-associated material (MAM) at the apical end of the released merozoites. In the 3D7 parasite SURFINs are encoded by 10 surface-associated interspersed (*surf*) genes, which are located close or within the subtelomeric region of five chromosomes. Frequent recombination events in this area are responsible for the considerable variability of proteins encoded in this region, also observed in SURFINs. N-terminally, SURFINs contain a cysteine rich domain (CRD) defined by six conserved cysteine residues, five of which are found positionally conserved in PvSTP1. The CRD precedes a region of high size and sequence variability, followed by a putative transmembrane (TM) region. In contrast to the variable N-terminal region, the C-terminal domain of SURFINs is relatively conserved and characterized by tryptophane rich domains (WRD) of approximately 150 amino acid residues, separated by less conserved sequences [20]. The WRDs establish a structural link to several *Plasmodium* surface proteins, i.e. PfEMP1, *Pk*SICA*var* and also the giant erythrocyte membrane protein 332 (Pf332), of which recent data also suggests surface exposure [21].

The objectives of the study were to analyze the $surf_{4.1}$ gene structure to determine whether it is a pseudo gene, as previously annotated, or a complete functional gene. The transcription pattern of the $surf_{4.1}$ gene and localization of $SURFIN_{4.1}$ on the protein level were also investigated.

Methods

Parasites and cultures

Parasites 3D7AH1, 3D7S8, FCR3, FCR3S1.2, 7G8 and TM180 were maintained in continuous culture according to standard procedures [22,23].

Analysis of surf gene presence and sequence heterogeneity in various parasite lines

Based on the 3D7 sequences of the annotated SURFINs, two sets of forward and reverse primers (Primer set 1 and Primer set 2), were designed for each *surf* gene. Some of the primers were designed to cross introns while others were within the open reading frames (ORFs) (Additional Files 1 and 2). Genomic DNA was extracted from trophozoite stages of 3D7S8, NF54, 7G8, DD2, FCR3, FCR3S1.2, TM284, TM180, R29, UAM25, UKS03, and UKS05 using the DNeasy Blood and Tissue kit according to the manufacturer's instructions (Qiagen, USA). Using two sets of independently designed *surf* gene specific primers, DNA was PCR amplified from each parasite. The following were the PCR conditions 35 cycles of 94°C for 30 sec, 55°C for 30 sec, and 68°C 60 sec.

$surf_{4.1}$ *transcript analysis*

Highly synchronized 3D7S8 and FCR3 parasites were harvested post invasion (p.i.) at early ring (10 h), late ring (20 h), early trophozoite (30 h), and schizont (40 h) parasite stages. The parasites were resuspended in pre-warmed TRIzol (Invitrogen, USA) (37°C) and incubated at 37°C for 5 minutes. Total RNA was extracted using the manufacturer's instructions (Invitrogen, USA) and DNAse treated (Ambion, USA). The RNA (100 ng) was reverse

transcribed (RT+) using MuLV reverse transcriptase enzyme and random hexamers (Applied Biosystems, USA) according to manufacturer's instructions. For each RT+ experiment, one RT- reaction (with reverse transcriptase omitted) was performed to ensure that there was no DNA contamination in the RNA.

surf$_{4.1}$ is currently present as PFD0100c in GeneDB, and PlasmboDB v5.4 but it was previously indicated as a truncated gene in the PlasmoDB v4.3 malaria database and was then suggestively comprised two distinct genes PFD0105c and PFD0100c. Primers (*surf*C$_{4.1}$F/R and Sintra$_{4.1}$ F/R) were consequently designed on opposite sides of the intergenic region of the two previously annotated genes (yielding amplification products of 1160 bp and 450 bp respectively, see Additional File 2). cDNA from ring stages, trophozoite stages and schizont stages was amplified using *surf*C$_{4.1}$F and *surf*C$_{4.1}$R. The RT-PCR cycling conditions were as follows: 35 cycles of 94°C for 30 sec, 55°C for 30 sec, and 68°C 60 sec. The cDNA from the different parasite stages was also amplified using primers specific to the *surf*$_{4.1}$ gene sections, these included 5CS-1F/R, 5CS-2F/R, *surf*C$_{4.1}$F/R, S$_{4.1}$F/R, 1C-S1F/R, 1C-S2F/R and 1C-S3F/R (Additional File 2).

Identification of the PFD0105c intron location

PCR was conducted using primers *surf*C$_{4.1}$F/R (Additional File 2) that were designed to cross the intergenic region and at the same time also read through the intron of the first part of the *surf*$_{4.1}$ gene (PFD0105c). The primers were used to amplify cDNA and gDNA from FCR3S1.2, 3D7S8, and NF54. The cDNA and gDNA PCR products were cloned into TOPOII vector (Invitrogen USA) and prepared for sequencing using the BigDye v3.1 kit (Applied Biosystems, USA) according to manufacturer's instructions.

Northern blot analysis

A fragment of *surf*$_{4.1}$, *surf*$_{4.1}$-C2 was PCR amplified using GWS$_{4.1}$F2, 5'- atcgagctcGTACTGAACCAAAACATCAT-3' and GWS$_{4.1}$R2, 5'-gatctcgagTGAATTAACGCTTCT-TCTAGT-3' primers from parasite DNA and cloned into TOPOII vector. After sequence confirmation, labelling was performed using vector specific M13Reverse, GWSF2 and T6/T7 DIG labelling kit (Roche, Germany) according to manufacturer's instructions. Total RNA from early rings (10 h), late rings (20 h) early trophozoite (30 h), and schizonts (40 h) were subjected to agarose gel electrophoresis and transferred to a nitrocellulose membrane (0.45 μm) (BIORAD, USA). The subsequent methodology was performed as described previously [20].

Sera and specific antibodies

A fragment of *surf* $_{4.1}$ (from the non-cytoplasmic part of the protein), SURFIN$_{4.1}$-C1 was PCR amplified from 3D7S8 using primers 5'-atcgagctcTTGGATAATACAGGT-GAT-3' and 5'-gatctcgagTTCCTTATGATGTTTTGGT-3'. The amplified DNA was cloned into TOPOII vector and sequenced. The SURFIN$_{4.1}$-C1 fragment was subsequently cloned into the PQE Trisystem -His strep 2 expression vector (Qiagen, USA) which adds a stretch of 6 histidine residues to the C terminus and 8 streptavidin residues at the N-terminus. The fusion protein was purified on His-Trap columns (Amersham Biotec, Sweden) charged with Nickel ions (1 M, $NiCl_2$, SIGMA, USA) according to manufacturer's instructions. The purified fusion protein was used to immunize rabbits (500 μg/injection) and rats (100 μg/injection) in Freund's complete adjuvant (SIGMA, USA) and boosted three times at one-month intervals with the same protein concentration in Freund's incomplete adjuvant. The animals were bled 10 days after the last boost.

Western blot analysis

Late stage FCR3 and 3D7S8 pRBCs from ≈32 h onwards were lysed in SDS sample buffer. Extracts (5 × 10^7 cells/lane) were separated on a 4–15% gradient SDS- PAGE (BIORAD). Proteins were transferred onto nitrocellulose membranes (0.45 μm) (BIORAD) and transiently stained with 0.1% Ponceau S in acetic acid. The membranes were blocked with 5% milk-PBS-0.05%Tween20 overnight (O/N) at 4°C, and then incubated with rabbit-anti-SURFIN$_{4.1}$-C1 purified IgG, polyclonal antibodies (1:200) in blocking buffer O/N at 4°C. Goat-anti-rabbit Ig coupled to alkaline phosphatase (1:10,000, Amersham Biotech, Sweden) was used as secondary antibody and the protein was visualized using 5-bromo-4-chloro-3-indolyl phosphate/nitroblue tetrazolium (BCIP/NBT) (SIGMA) in water.

Real-time quantitative PCR analysis of surf$_{4.1}$ copy numbers and transcription levels

Copy numbers of *surf*$_{4.1}$ were determined for 7G8, 3D7AH1, FCR3 and their daughter clones 3D7S8 and FCR3S1.2. Genomic DNA (gDNA) was prepared using Easy-DNA™ Kit (Invitrogen) as previously described [17]. In addition, transcriptional levels were analysed for 3D7S8 and FCR3. Parasites were kept tightly synchronized using 5 % (w/v) sorbitol, and were harvested at 4 h post invasion intervals for two consecutive parasite generations. RNA from each time point was isolated using the RNeasy® Mini Kit according to the manufacturer's instructions and contaminating gDNA was removed using the RNase-Free DNase Set (Qiagen). Total RNA was reversely transcribed with SuperScript III RNase H reverse transcriptase (Invitrogen), with random hexamers and oligo(dT)$_{12-18}$ (300 ng/ml and 25 ng/ml respectively; Invitrogen) at 50°C for two hours. For each cDNA synthesis reaction, a control reaction without reverse transcriptase (RT-) was performed with identical amounts of template. For real-time quantitative PCR (Rt-QPCR) determination

of copy numbers as well as to monitor relative transcription of $surf_{4.1}$ to the endogenous control *seryl-tRNA synthetase*, the primers $surf_{4.1}$ were employed:

5'-TTTGAAGCTCCTGGTCAAGGA-3', $surf_{4.1}$-3': TTGTTTGTGCAAGTGTTTTGAAAG, PF07_0073-5': TATCATCTCAACAGGTAT CTACATCTCCTA and PF07_0073-3': TTTGAGAGTTACATGTGGTATCATCTTTT. These primers as well as the complete Rt-QPCR amplified product were designed to conserved regions in the parasite lines studied. Amplification efficiencies of the primer pairs were tested on dilution series of both gDNA and cDNA from all parasites, and were proven sufficiently close (ranging from 94.4 to 99.2%) to obviate the need for a correction factor. Amplification reactions for both relative copy numbers (gDNA) and relative transcription (cDNA) were done in quadruplicate in 20 μl, containing Power SYBR Green master mix (Applied Biosystems), 300 nM of each forward and reverse primer and 2 ng of template. Forty five cycles (95°C for 15 sec and 60°C for 1 min) were performed in an ABI sequence detector 7500 (Applied Biosystems). Relative copy numbers were analysed according to the ΔΔCt method and plotted using SigmaPlot 9.0 (Systat Software Inc.). Transcription levels were achieved by dividing log-transformed Ct values ($2^{-\bar{x}\ Ctsurf4.1}$ / $2^{-\bar{x}\ Cteryl\text{-}tRNA\ synthetase}$) for each strain and time point (for details see Additional File 6). The standard deviation of the quotient was calculated according to the User Bulletin 2, Applied Biosystems. Results were visualized as log_2 transformed values plotted using SigmaPlot 9.0 (Systat Software Inc.).

Indirect immunofluorescence on air-dried monolayers and localization of $SURFIN_{4.1}$

For immunofluorescence assays (IFA), monolayers of pRBCs were prepared as previously described [24]. Monolayers were incubated with rabbit anti-$SURFIN_{4.1}$-C1 antibody (1:400) or pre-immune serum for 30 min at room temperature and subsequently with a secondary anti-rabbit Alexa 488 (1:100; Jackson, USA) for 30 min. The cells were then incubated with propidium iodide (1:100) for nuclear staining for 30 min. Preparations were washed three times with PBS between each antibody preparation.

In the co-localization assay with EBA175, monolayers were incubated with rabbit anti-$SURFIN_{4.1}$-C1(1:100) for 30 min and thereafter with anti-rabbit -TRITC (1:100, Jackson, USA) for another 30 min. Monolayers were then probed with rat anti-EBA175 (MR-2) (1:400; ATCC/MR4) and after three washes with PBS probed with secondary anti-rat Alexa 488 antibody.

When $SURFIN_{4.1}$ was evaluated for its co-localization with $SURFIN_{4.2}$ and MSP1, monolayers were probed with rat anti-$SURFIN_{4.1}$-C1 (1:100) for 30 min, washed three times and incubated with secondary chicken-anti-rat Alexa 488 for 30 min. The monolayers were then incubated with rabbit anti-$SURFIN_{4.2}$ (1:200) or rabbit anti-MSP1 FVO (1:400, ATCC/MR4) for 30 min and then probed with secondary goat-anti-rabbit Ig- TRITC (1:100; Jackson, USA) for 30 min. HOESCHT and/or DAPI (Jackson, USA) were used for nuclear staining. All incubations were carried out at room temperature in a humid chamber. Slides were analysed with a Nikon Optiphot 2 UV microscope.

Agglutination assays

To analyse the ability of the immune anti-$SURFIN_{4.1}$-C1serum to agglutinate pRBCs, synchronized parasite cultures of 3D7S8 and FCR3 were incubated with serum as described by Barragan *et al* [25]. The samples were then analysed under the microscope for presence of clumps or agglutinates. Acridine orange was used for staining of the parasite.

Results

The data presented here shows a revised gene structure of $surf_{4.1}$, which combines two previously identified open reading frames (PFD0100c and PFD0105c) (plasmodb.org v4.3 and Figure 1A). This was obtained by bioinformatic analysis and confirmed by PCR, which shows that $surf_{4.1}$ is one complete gene with three exons separated by two introns (Figure 1B). In PlasmoDB, $surf_{4.1}$ gene was previously annotated as two individual open reading frames, PFD0100c and PFD0105c separated by a 410 bp intergenic region (hereby referred to as intergenic region). However, RT-PCR amplification using primers designed to amplify the fragment surrounding this intergenic region, showed a single band from cDNA indicating that the annotation was incorrect and that these two predicted open reading frames compose a single open reading frame. This led to the recent re-annotation of the gene in PlasmoDB v5.4. In this study the $surf_{4.1}$ transcript was shown to be a single open reading frame in 3D7S8, FCR3, FCR3S1.2, 3D7AH1, 7G8 and TM180 parasite lines (Figure 1B).

$surf_{4.1}$ and other surf genes exhibit sequence heterogeneity in laboratory parasites and field isolates

The presence of $surf_{4.1}$ in laboratory strains and clinical isolates was investigated. PCR on gDNA with $surf_{4.1}$ specific primers resulted in specific amplification in all parasite lines (Additional File 3). The remaining *surf* genes were also amplified, some with only one primer set while

Figure 1. A

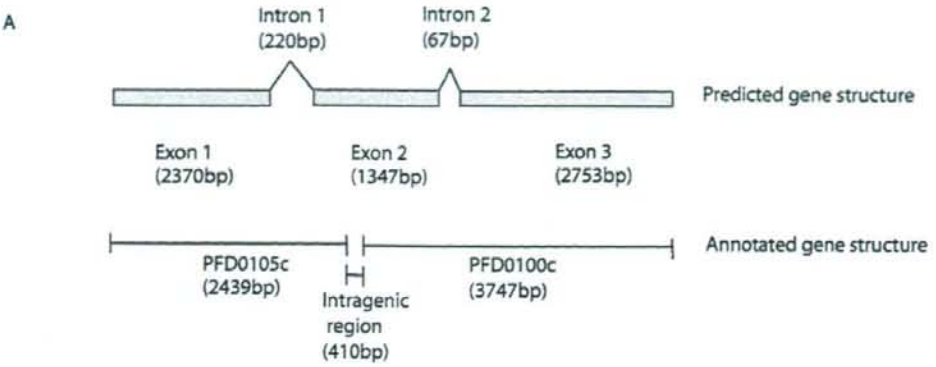

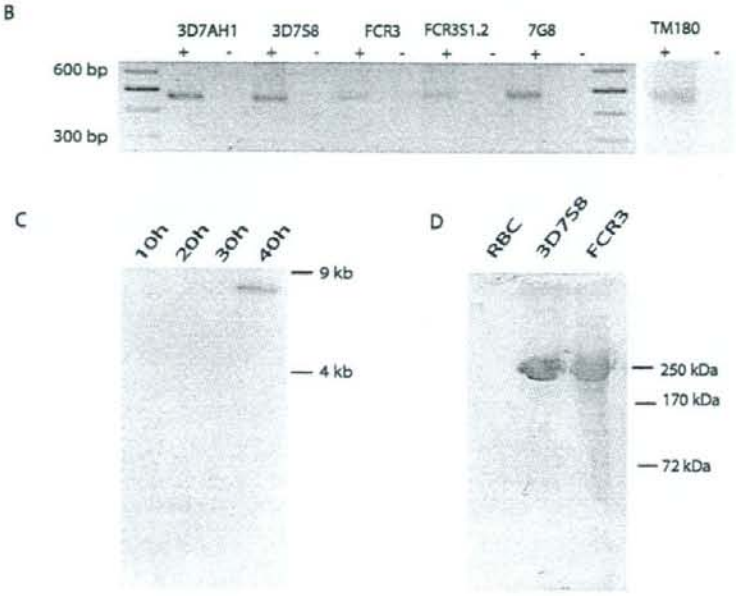

Figure 1

***surf*$_{4.1}$ from gene to protein**. A). The new *surf*$_{4.1}$ gene structure, showing three exons separated by two introns. Previously the gene was annotated as two genes (PFD0100c and PFD0105c). Using the new structure, with the two genes combined, the protein structure of SURFIN$_{4.1}$ is estimated to be a 258.3 kDa protein. B). PCR with Sintra$_{4.1}$F/R primers amplified the intergenic region separating the two genes which make up *surf*$_{4.1}$ (PFD0105c and PFD0100c). PCR on cDNA shows presence of transcript in 3D7AH1, 3D7S8, FCR3, FCR3S1.2, 7G8, and TM180 parasite strains. + and - indicate cDNA treated with reverse transcriptase (+) and one not treated with reverse transcriptase (-) respectively. C). Northern blot on 3D7S8, 10 hrs, 20 hrs, 30 hrs and 40 hrs RNA with *surf*$_{4.1}$ specific probe. A band of an approximately 7 kb is observed from RNA extracted at 40 h post invasion. The *surf*$_{4.1}$ RNA has an open reading frame with a spliced size of 6471 bp. D). Immunoblot on whole parasite cultures of 3D7S8 and FCR3 from 40 hrs^{+} probed with rabbit anti-SURFIN$_{4.1}$ purified IgG show a band above 250 kDa confirming that SURFIN$_{4.1}$ is a full protein encoded by a complete *surf*$_{4.1}$ gene.*surf* $_{4.1}$ gene encodes a protein estimated at 258.3 kDa.

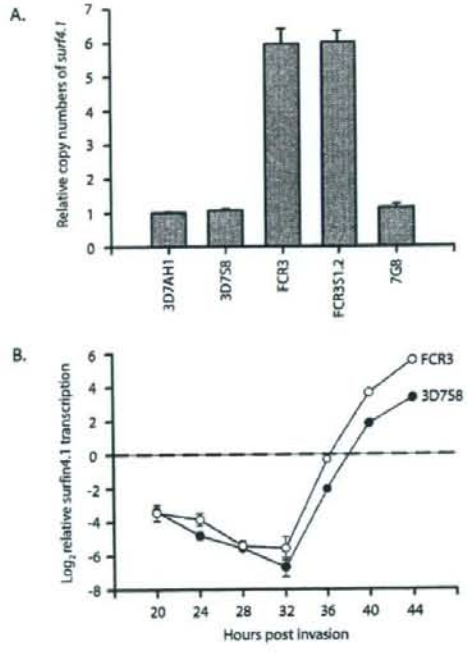

Figure 2
***surf*$_{4.1}$ copy numbers and transcription pattern.** A). Rt-QPCR analysis of *surf*$_{4.1}$ copy numbers in 3D7AH1, 3D7S8, FCR3, FCR3S1.2 and 7G8 parasite strains revealed FCR3 and FCR3S1.2 to have six copies relative to the other strains. The relative copy number determination was conducted using *seryl-tRNA synthetase* as the endogenous control gene. B). Rt-QPCR reveals that *surf*$_{4.1}$ transcription is initiated at ≈32 h post invasion and peaks during late schizogony. FCR3 shows ≈5-fold higher level of transcription compared to 3D7S8 at 44 h post invasion, corresponding well to the gene copy number abundance in respective genomes. Results are visualized as $\log_2$ transformed values.

others were amplified using two primer sets. These two separate primer sets were used to account for any sequence differences and to ensure that as many *surf* genes were amplified from the different parasites. Genomic DNA sequences from 3D7, HB3, D10, DD2 and 7G8 from *surf*4.1 (1–2320 bp.) showed sequence polymorphisms within the parasite isolates (Additional File 4).

surf$_{4.1}$ exists in different copy numbers in different parasite strains

Six copies of *surf*$_{4.1}$ gene were observed in FCR3 and its daughter clone FCR3S1.2 and one copy in each of 3D7AH1, 3D7S8, and 7G8 (Figure 2A and Additional File 5). Achieved copy numbers confirm previous findings where microarray and fluorescent *in situ* hybridizations were used for quantification [18].

surf genes are differentially transcribed dependent on developmental stage and strain

To understand the transcription patterns of the *surf* genes in the 3D7S8 parasite clone, RT-PCR was performed with primers specifically targeting individual sequences of all 10 *surf* genes (Additional File 1). Different *surf* genes were found expressed at different times during the erythrocytic cycle (Table 1). *surf*$_{1.3}$, *surf*$_{4.2}$ and *surf*$_{8.3}$ were expressed throughout the cycle, from the early rings to the schizonts, while other *surf* genes were either not detected (*surf*$_{1.2}$, *surf*$_{8.1}$, *surf* $_{8.2}$ and *surf*$_{13.1}$) or restricted to later trophozoites and/or schizont development (*surf*$_{1.1}$, *surf*$_{4.1}$ and *surf*$_{14.1}$) (Table 1). *surf*$_{4.1}$ was found prominently transcribed in late stages in the two parasite lines 3D7S8 and FCR3, with an apparent onset of transcription at ≈32 h and peaking in late schizonts (Figure 2B and Additional File 6). An obvious difference in transcript levels was observed between these two parasite lines, corresponding to the difference in copy numbers of the *surf*$_{4.1}$ gene.

The transcription pattern of *surf*$_{4.1}$ was confirmed with Northern blot experiments using specific probes. *surf*$_{4.1}$ mRNA of approximately 9 kB was detected in schizonts > 40 h post infection (Figure 1C).

Identification of SURFIN$_{4.1}$ *by immunoblotting*

Immunoblot analysis was performed with SDS-lysates obtained from synchronized *in vitro* cultures of 3D7S8 and FCR3. Using polyclonal rabbit-anti-SURFIN$_{4.1}$-C1 antibodies, a band of approximately 250 kDa was detected in schizont stage parasites (36–40 h), which corresponds to the predicted SURFIN$_{4.1}$ protein mass of 258 kDa (Figure 1D). Similar intensities were observed in both FCR3 and 3D7S8. Achieved data is consistent with the RT-PCR analysis suggesting PFD0100c and PFD0105c to form a single open reading frame.

SURFIN$_{4.1}$ *is localized to the parasitophorous vacuole (PV)*

To study the localization of SURFIN$_{4.1}$, IFA was carried out on 3D7S8 and FCR3 air-dried monolayers using purified rabbit-anti-SURFIN$_{4.1}$-C1 IgG. SURFIN$_{4.1}$ was found expressed during the mature stages of the parasite (30 h and onwards, Figure 3). There was no recognition of SURFIN$_{4.1}$ during the early ring stages (0–16 h) or in trophozoite stages (16–24 h). In the late trophozoite stages (25–30 h) SURFIN$_{4.1}$ was observed close to the food vacuole (FV) in the PV as a distinct spot, which later spread out within the PV in a dotty pattern (Figure 4) in both 3D7S8 and FCR3.

During late schizont stage, SURFIN$_{4.1}$ was seen as merozoite associated material (MAM) around the newly